

TA7
W34
no. SL-96-10
c. 3



Technical Report SL-96-10
June 1996

**US Army Corps
of Engineers**
Waterways Experiment
Station

US-CE-C Property of the
United States Government

Dynamic Analysis of the American Maglev System

by Yazmin Seda-Sanabria, James C. Ray

Approved For Public Release; Distribution Is Unlimited

**Research Library
US Army Engineer Waterways
Experiment Station
Vicksburg, Mississippi**

Prepared for U.S. Army Engineer Division, Huntsville

35133510

Technical Report SL-96-10
June 1996

TA7
W34
No. SL-96-10
C.3

Dynamic Analysis of the American Maglev System

by Yazmin Seda-Sanabria, James C. Ray

U.S. Army Corps of Engineers
Waterways Experiment Station
3909 Halls Ferry Road
Vicksburg, MS 39180-6199

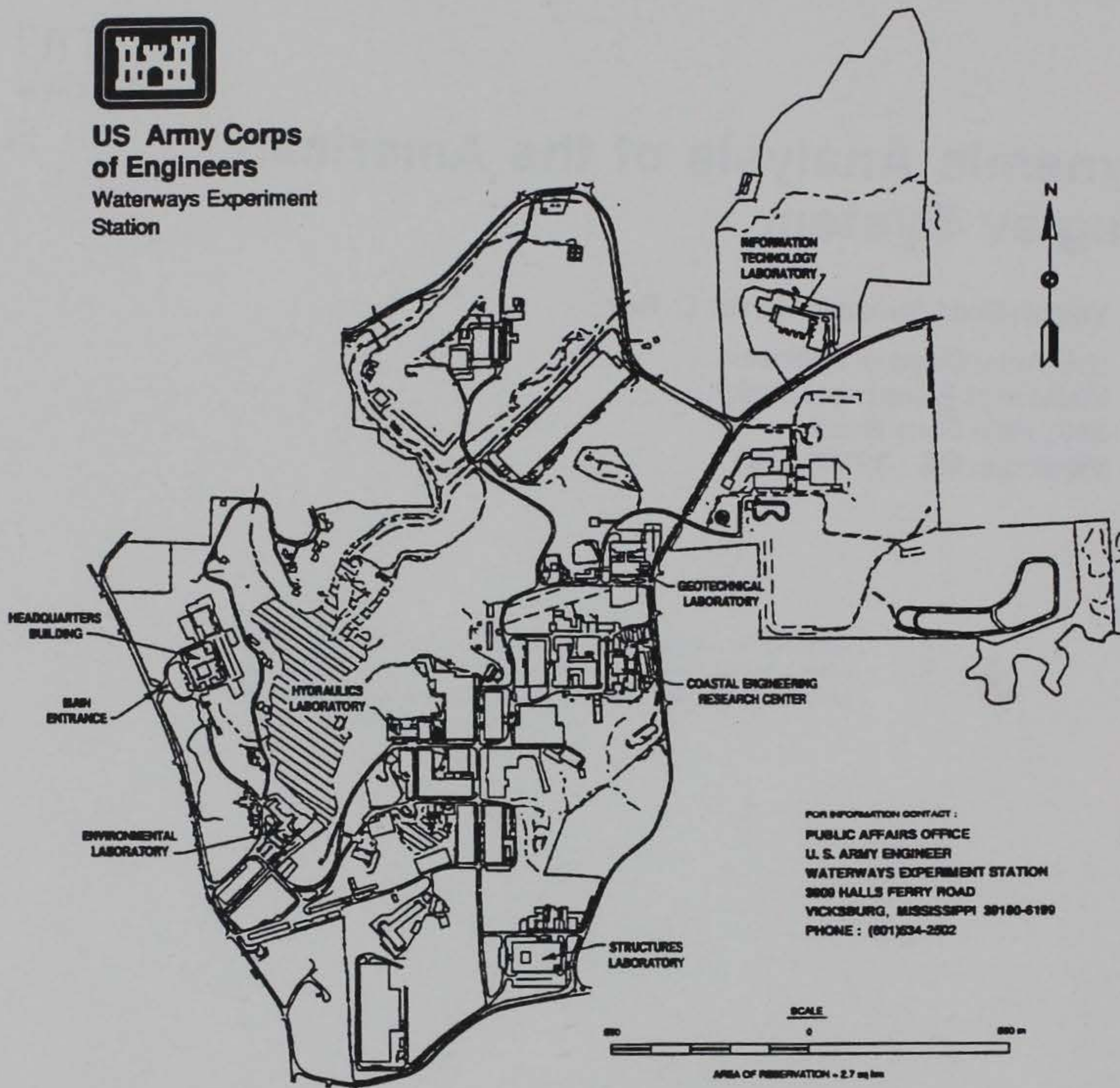
Final report

Approved for public release; distribution is unlimited

Prepared for U.S. Army Engineer Division, Huntsville
P.O. Box 1600, Huntsville, AL 35807-4301



**US Army Corps
of Engineers**
Waterways Experiment
Station



FOR INFORMATION CONTACT:
PUBLIC AFFAIRS OFFICE
U. S. ARMY ENGINEER
WATERWAYS EXPERIMENT STATION
3809 HALLS FERRY ROAD
VICKSBURG, MISSISSIPPI 39180-6199
PHONE: (601)834-2502

Waterways Experiment Station Cataloging-in-Publication Data

Seda-Sanabria, Yazmin.

Dynamic analysis of the American Maglev System / by Yazmin Seda-Sanabria, James C. Ray ; prepared for U.S. Army Engineer Division, Huntsville.

61 p. : ill. ; 28 cm. — (Technical report ; SL-96-10)

Includes bibliographic references.

1. Magnetic levitation vehicles — Analysis. 2. High speed ground transportation — Analysis. I. United States. Army. Corps of Engineers. Huntsville Division. II. U.S. Army Engineer Waterways Experiment Station. III. Structures Laboratory (U.S. Army Engineer Waterways Experiment Station) IV. Title. V. Series: Technical report (U.S. Army Engineer Waterways Experiment Station) ; SL-96-10.

TA7 W34 no.SL-96-10

Contents

Preface	vi
Conversion Factors, Non-SI to SI Units of Measurement	vii
1—Introduction	1
Background	1
Objective	2
Scope	2
2—System Description	3
Guideway	3
Vehicle	3
3—Finite Element (FE) Analysis	10
FE Methodology	10
Guideway Mesh	11
Vehicle Mesh	12
Slidelines	15
Dynamic Analysis	16
4—Analytical Results	17
5—Conclusions and Recommendations	29
References	31
Appendix A: ABAQUS Input File	A1

List of Figures

Figure 1.	Details of guideway structure for American Maglev SCD	4
Figure 2.	Plan view of vehicle's lift sites	5
Figure 3.	Vehicle of the American Maglev SCD	6
Figure 4.	Variation of active lift force with vertical displacement .	6
Figure 5.	Active lift coil offset for stable levitation	7
Figure 6.	Nonlinear stiffness variation	8
Figure 7.	Composite coil lift force for various speeds	9
Figure 8.	American Maglev SCD guideway mesh	11
Figure 9.	American Maglev SCD vehicle mesh	13
Figure 10.	Variation of active lift force with displacement	15
Figure 11.	Vertical displacement of midspan 1 (linear spring only)	19
Figure 12.	Vertical displacement of midspan 1 (both springs)	19
Figure 13.	Vertical displacement of midspan 2 (linear spring only)	20
Figure 14.	Vertical displacement of midspan 2 (both springs)	20
Figure 15.	Vertical displacement of midspan 5 (linear spring only)	21
Figure 16.	Vertical displacement of midspan 5 (both springs)	21
Figure 17.	Vertical displacement of vehicle's front (linear spring only)	22
Figure 18.	Vertical displacement of vehicle's front (both springs)	22
Figure 19.	Vertical displacement of vehicle's rear (linear spring only)	23
Figure 20.	Vertical displacement of vehicle's rear (both springs)	23
Figure 21.	Vertical acceleration of vehicle's front (linear spring only)	24

Figure 22.	Vertical acceleration of vehicle's front (both springs)	24
Figure 23.	Vertical acceleration of vehicle's rear (linear spring only)	25
Figure 24.	Vertical acceleration of vehicle's rear (both springs)	25
Figure 25.	Spring force at vehicle's front (both springs)	26
Figure 26.	Spring force at vehicle's rear (both springs)	26
Figure 27.	Magnetic gap variation at vehicle's front (linear spring only)	27
Figure 28.	Magnetic gap variation at vehicle's front (both springs)	27
Figure 29.	Magnetic gap variation at vehicle's rear (linear spring only)	28
Figure 30.	Magnetic gap variation at vehicle's rear (both springs)	28

Preface

The research reported herein was sponsored by the U.S. Army Engineer Division, Huntsville. Mr. Rick Suever was the Program Monitor, and Dr. John Potter was the Technical Monitor.

All work was carried out by Ms. Yazmin Seda-Sanabria and Mr. James C. Ray, Structural Mechanics Division (SMD), Structures Laboratory (SL), U.S. Army Engineer Waterways Experiment Station (WES), under the general supervision of Mr. Bryant Mather, Director, SL; Mr. John Ehrgott, Assistant Director; and Dr. Reed Mosher, Chief, SMD.

At the time of publication of this report, Director of WES was Dr. Robert W. Whalin. Commander was COL Bruce K. Howard, EN.

The contents of this report are not to be used for advertising, publication, or promotional purposes. Citation of trade names does not constitute an official endorsement or approval of the use of such commercial products.

Conversion Factors, Non-SI to SI Units of Measurement

Non-SI units of measurement used in this report can be converted to SI units as follows:

Multiply	By	To Obtain
feet	0.3048	metres
inches	25.4	millimetres
miles (U.S. statute)	1.609347	kilometres
pounds (force) per square inch	0.006894757	megapascals
pounds (mass)	0.4535924	kilograms
tons (2,000 pounds, mass)	907.1847	kilograms

1 Introduction

Background

Practical superconducting magnetic levitation (Maglev) was pursued in the United States in the 1960's. Development of the concept continued for a short time in the United States; but in the 1970's, Federal funding for Maglev vanished and development effectively ceased. Foreign governments, however, continued development of the Maglev concept. Today, both Germany and Japan have working prototypes.

As a result of the evolving foreign technology and increasing transportation needs, the United States' interest in Maglev was renewed in 1990. In December 1990, the National Maglev Initiative (NMI) was formed in conjunction with the Department of Transportation, the Corps of Engineers, and the Department of Energy. Its purpose was to evaluate the potential for Maglev to improve intercity transportation in the United States and to determine the appropriate role for the Federal Government in advancing this technology. As part of its evaluation, the NMI formed an independent Government Maglev System Assessment (GMSA) team, composed of experts from both the Government and private industry. Its purpose was to assess the technical viability of potential U.S. Maglev system concept designs (SCD's). The Structural Mechanics Division (SMD), Structures Laboratory (SL), U.S. Army Engineer Waterways Experiment Station (WES), sponsored through the U.S. Army Engineer Division, Huntsville (HND), was part of this team and provided expertise in all areas related to the guideway structure and dynamic vehicle/guideway interaction (VGI). VGI refers to the dynamic interaction (coupling) between two separate dynamic systems: the Maglev vehicle and its supporting flexible guideway.

As a result of their work as part of the GMSA team, SMD developed a unique finite element (FE) analytical methodology for the study of VGI (Ray et al. 1995). The methodology has two distinct applications: it can be used to provide an estimate of the vehicle ride quality for a given vehicle and guideway design and to accurately predict the dynamic deflections and stresses experienced throughout the guideway structure as a result of a vehicle passage. Ride quality results are necessary to design a vehicle suspension system and to determine the guideway stiffness required to meet specific ride quality criteria.

Dynamic structural analyses are necessary to produce safe, economical, and accurate guideway designs.

As the United States interest in Maglev grew, many companies developed (through various funding sources) Maglev SCD's of their own. As a means of encouraging this type of development, HND provided technical support to some of these companies. One such company was American Maglev Technology, Inc. HND funded SMD, WES, to conduct a VGI analysis of their system using their FE analytical methodology. This report presents a summary of that work.

Objective

The objective of this work was to conduct a VGI analysis of the American Maglev System. Of particular interest in the study was a comparison of the ride quality of the vehicle using two different suspension designs and the resulting affects on the guideway structure.

Scope

The FE methodology for VGI analyses as described by Ray et al. (1995) was utilized for the study herein. The details of the American Maglev system were obtained from Grant (1994) and Davey (1994 and 1995a, b). All FE modeling was accomplished in two dimensions (2-D), since sufficient three-dimensional (3-D) response characteristics (such as vehicle roll and yaw inertias) were not available in the references.

In order to study the vehicular response over a significant length of guideway, a series of three two-span continuous sections of guideway were modeled; i.e., a total of six spans at (90 ft) each with continuous spans at every other support. Two different scenarios were studied for the vehicle: one scenario with both an active (nonlinear) suspension and a passive (linear) suspension acting together; and one with the passive suspension by itself. This comparison was made in order to show the effectiveness/need for the elaborate active suspension system. Separate analyses were made for both of these scenarios at vehicle forward velocities of (100, 200, and 300 mph). The results of these analyses are provided and compared in the form of data plots and are discussed in Chapter 4.

2 System Description

Guideway

The design details used in the modeling of the guideway are described by Grant (1994) and Davey (1995b). The guideway structure is depicted in Figure 1. The superstructure of the guideway is a two-span continuous composite structure comprised of two prestressed concrete (PSC) beams and one cast-in-place (CIP) concrete slab. The modulus of elasticity for the PSC beams is 4,888 ksi, while for the CIP slab is equal to 3,834 ksi. The moment of inertia of one PSC beam is equal to 632,636 in⁴. The transformed moment of inertia of the guideway is 1,999,784 in⁴.

The "railings" on which the vehicle is supported, propelled, and guided are attached to the top of the guideway structure. The railings are a 20.9-in.-high by 1.5-in.-wide sandwich of pulltruded fiberglass polyvinyl. They contain both the composite and active lift coils, as shown in Figure 2.

Vehicle

Details of the American Maglev SCD vehicle were obtained from Davey (1994, 1995a, b). The vehicle is depicted in Figure 3. It is (90 ft) long and weighs approximately 40 tons. As shown previously in Figure 2, there are four "lift sites" along the length of the vehicle and one lift site per side at each of these locations, making a total of eight lift sites. Each lift site consists of four "C set" magnet pairs spaced at 20-in. centers. Each C set magnet pair effectively wraps around the vertical coils on the guideway, as shown in Figure 3. The coils provide two mechanisms for realizing lift: an active lift coil and a composite (null flux) lift coil system. Together, they provide the interaction between the vehicle and the rail.

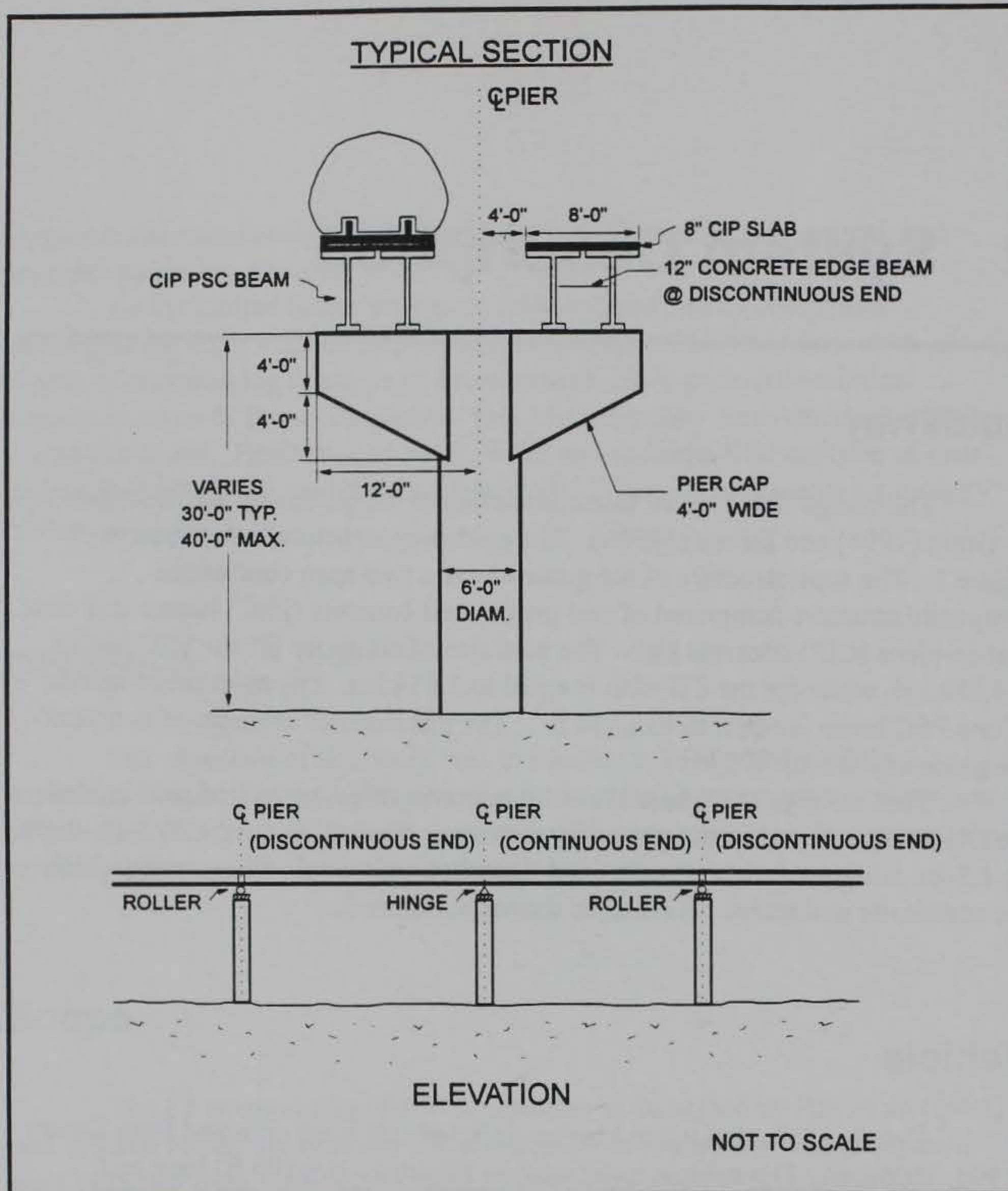


Figure 1. Details of guideway structure for American Maglev SCD

The lift force associated with the active lift coils is independent of the vehicle's speed and is defined by the following polynomial equation :

$$F_y (\text{tons}) = 0.0104y^3 - 0.1112y^2 - 0.0205y + 1.3998 \quad (1)$$

The variation of the active lift coil force, F_y , with the vertical displacement, y , is shown in Figure 4. The maximum lift will be obtained when the active lift coils are centered on the shadow of the magnet faces. However, as seen in Figure 4, this corresponds to an unstable position, since the spring constant (the slope of the curve of Figure 4) becomes zero at this displacement and assumes a negative value with slight perturbations. Therefore, the active lift coil has been given an initial offset of 1.5 in., as presented in Figure 5. The factor that drives the offset

is the margin of safety desired, or the "overburden." As seen in Figure 4, an offset distance of $y = 1.5$ in. corresponds to an overburden of 491 lb (0.245 ton). This reflects an 18-percent reduction in force from the peak achievable without any active current control (the peak lift force equals 2,800 lb per C set at 35,800 amps, and the suggested operating point yields a lift force of 2,308 lb per C set at 35,800 amps). The spring constant is the local slope, or the first

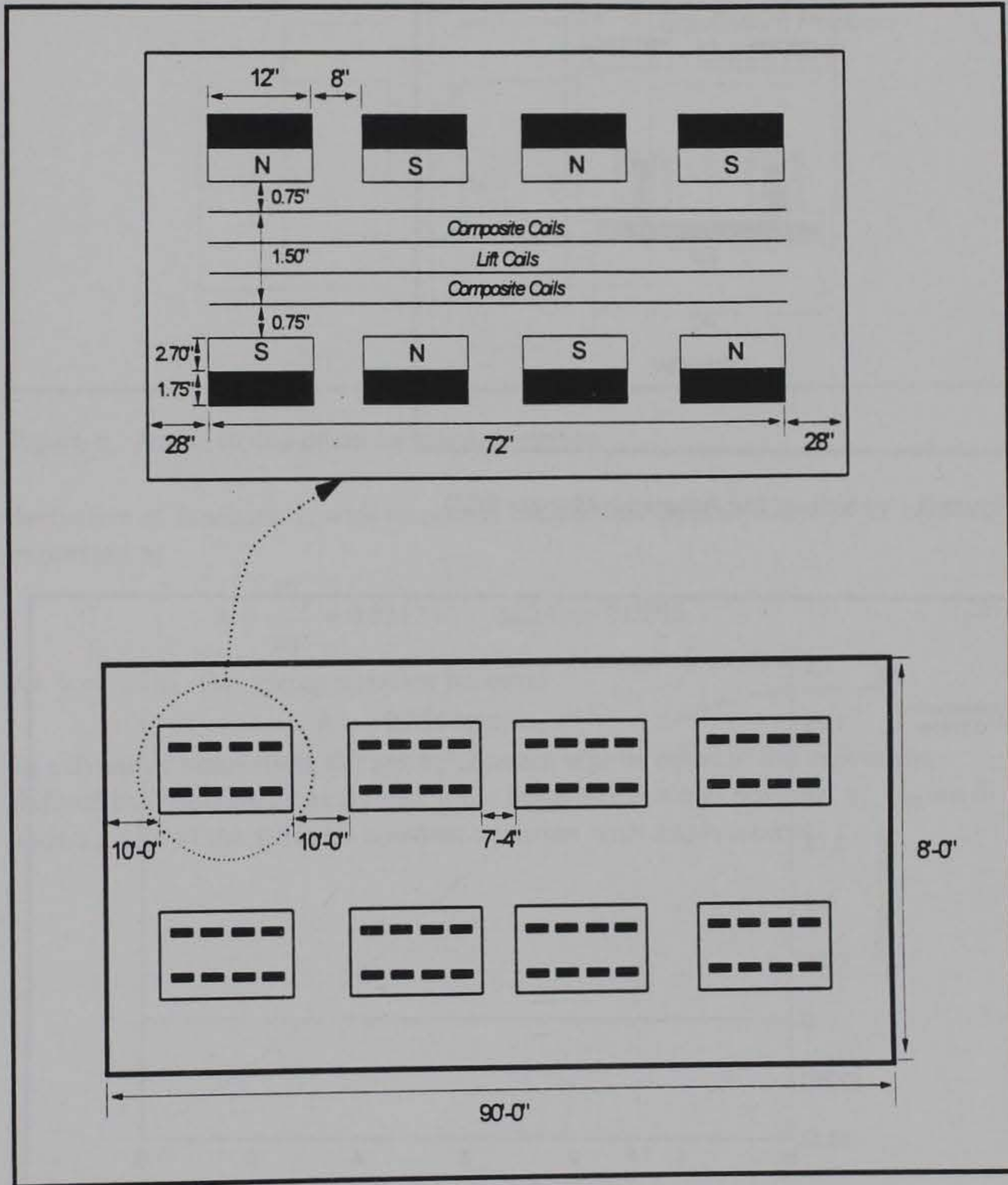


Figure 2. Plan view of vehicle's lift sites

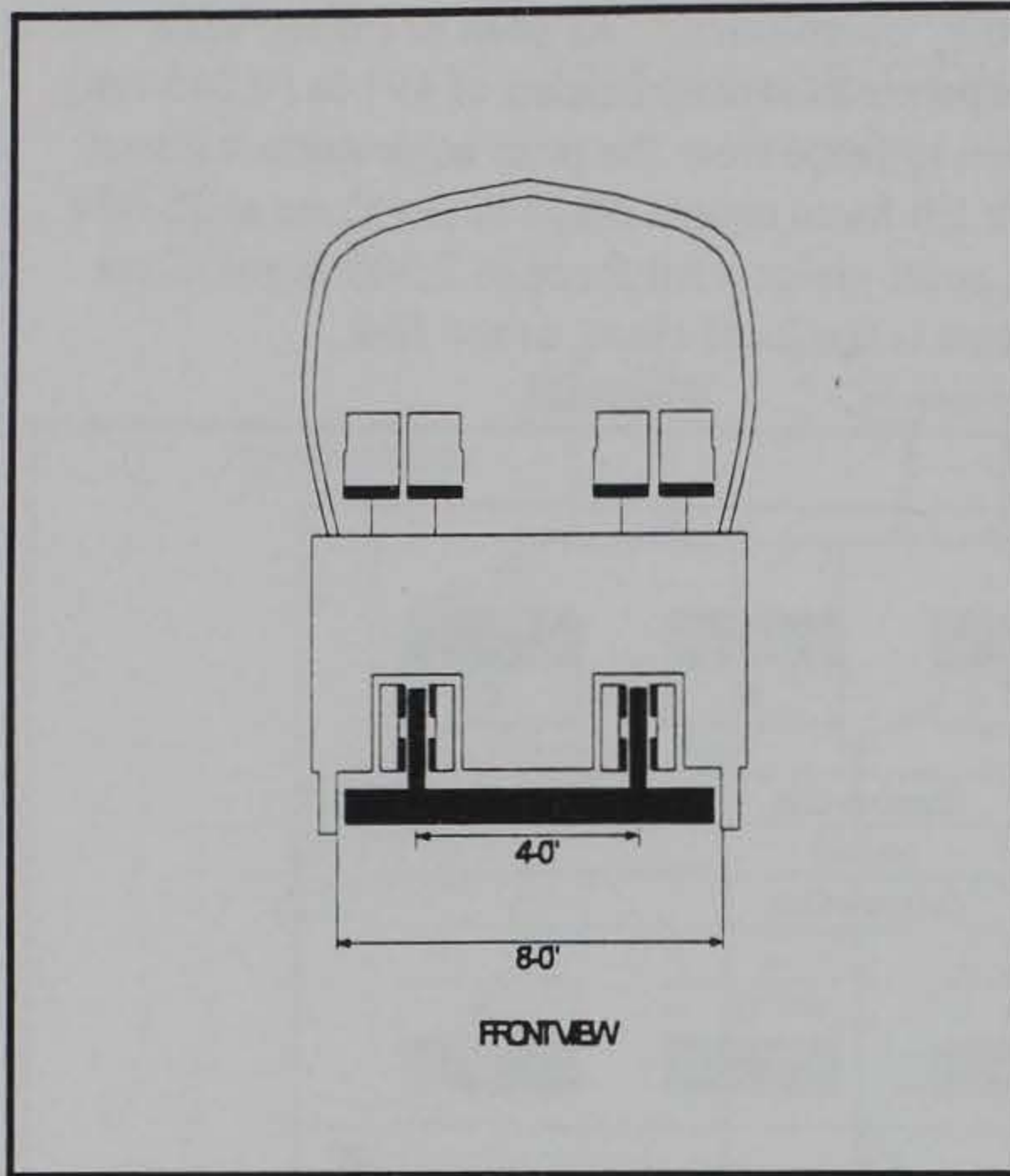


Figure 3. Vehicle of the American Maglev SCD

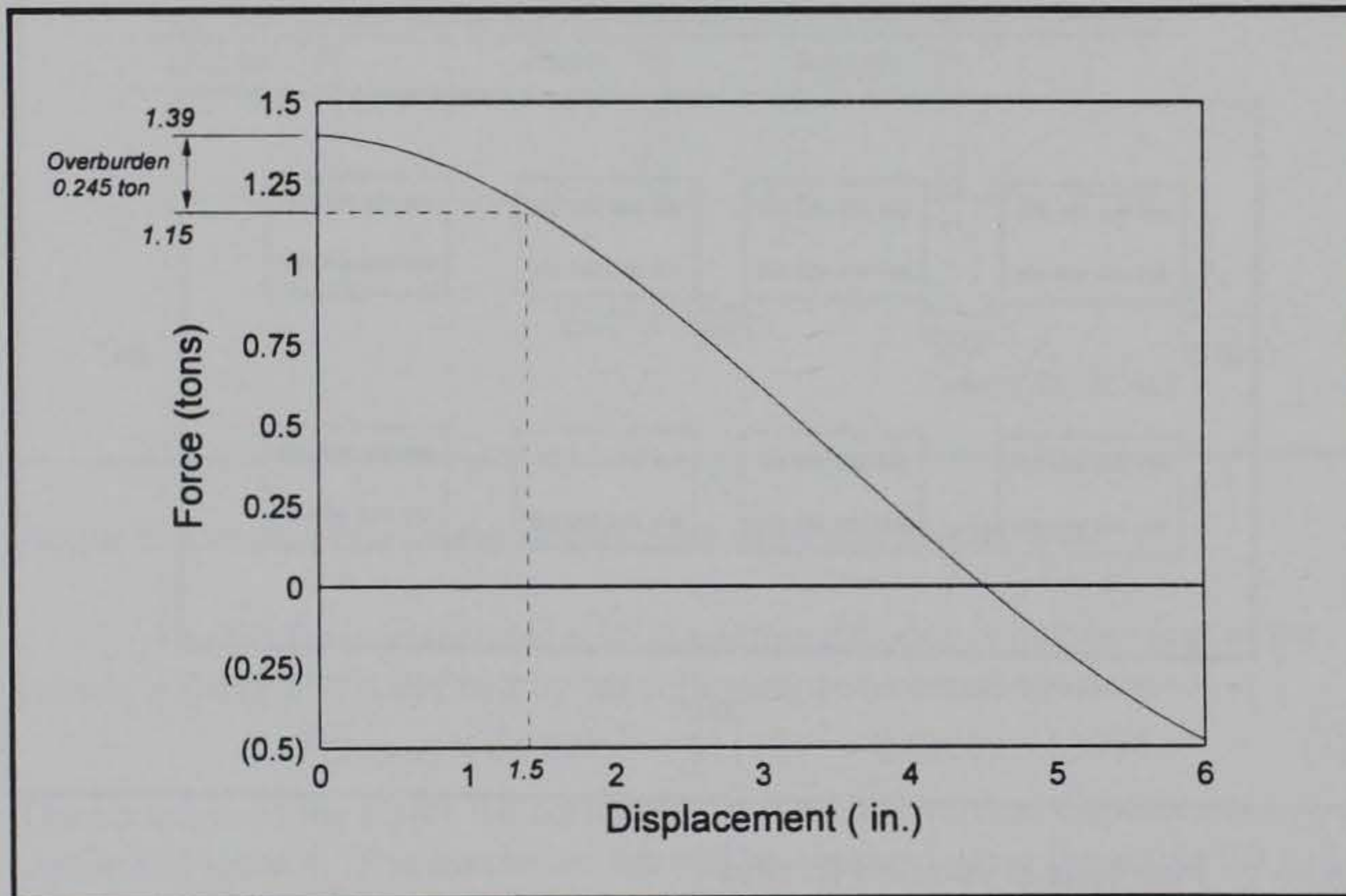


Figure 4. Variation of active lift force with vertical displacement

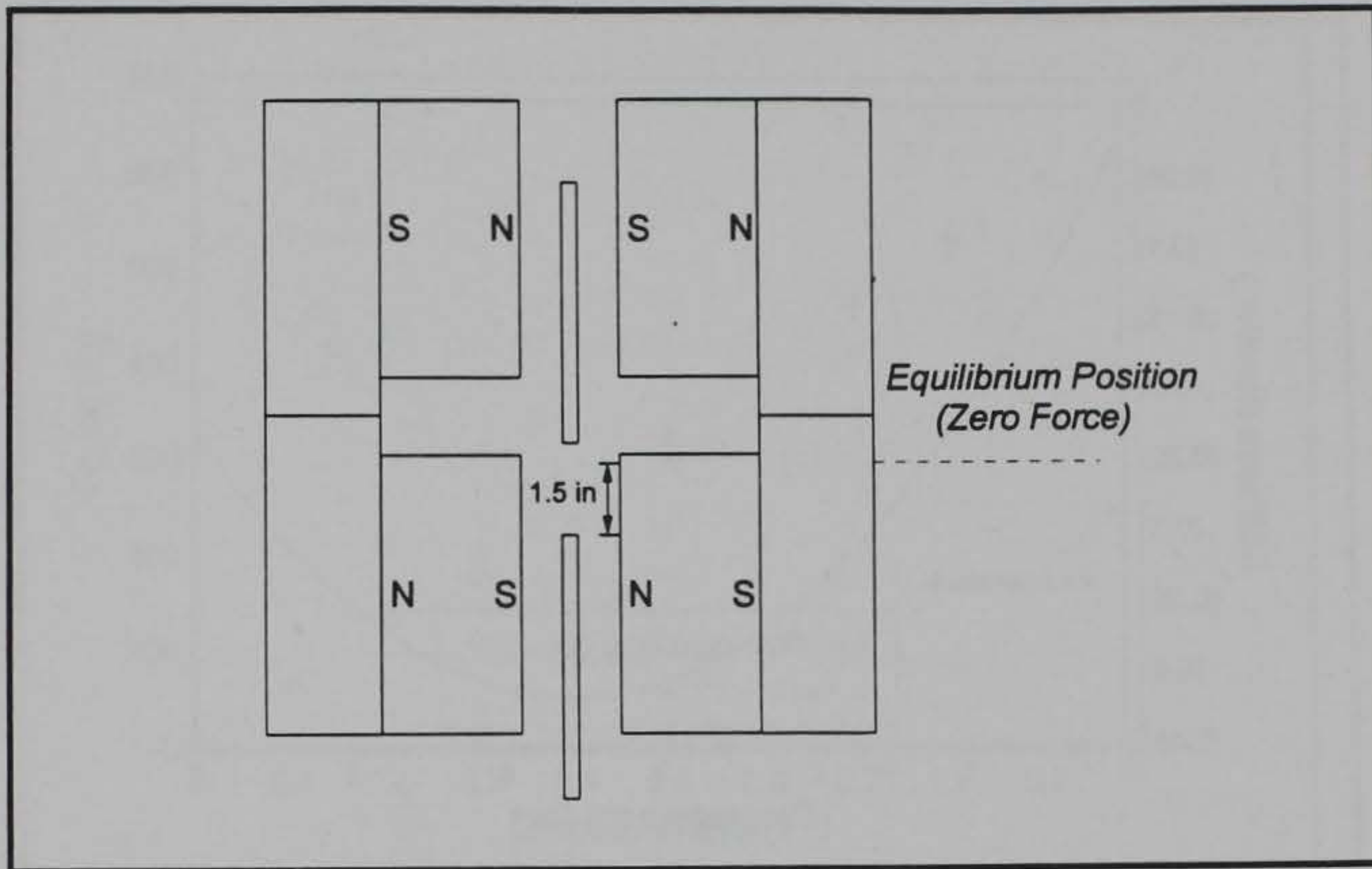


Figure 5. Active lift coil offset for stable levitation

derivative of Equation 1, with respect to the vertical displacement, y . It can be expressed as :

$$k = \frac{dF_y}{dy} = 0.0312y^2 - 0.224y - 0.0205 \quad (2a)$$

At $y = 1.5$ in., this spring constant becomes :

$$k = -0.284 \text{ tons/in.} \quad (2b)$$

In a dynamic simulation, the spring constant will be equal to the expression defined by Equation 2a evaluated at the instantaneous coil position, y . Figure 6 shows a plot of the stiffness constant variation with displacement.

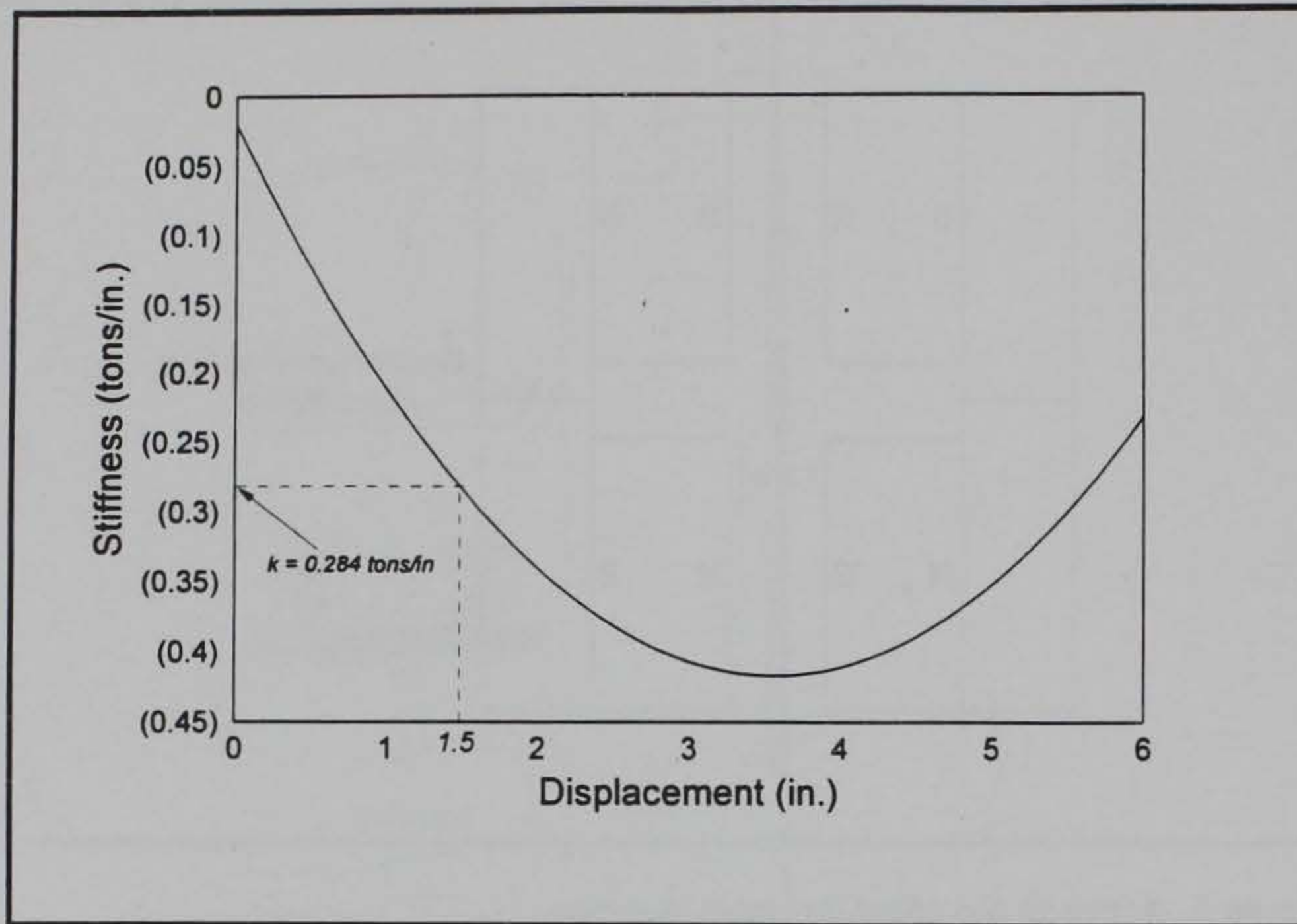


Figure 6. Nonlinear stiffness variation

As mentioned previously, there is also a secondary mechanism for realizing lift known as the composite (null flux) lift coils. The forces from these coils are superimposed on those from the active lift coils and can be simulated using a stationary winding excited at a frequency, ω . This frequency is related to the velocity of the vehicle according to this relationship :

$$\omega = k \cdot v \quad (\text{in rad/sec}) \quad (3a)$$

$$f = \frac{\omega}{2\pi} \quad (\text{in Hz}) \quad (3b)$$

Upon substitution in Equation 3b, the frequencies corresponding to velocities $v = 100$ -, 200 -, and 300 mph, respectively, are $f = 43.3$ -, 86.5 -, and 129.8 Hz, respectively. The composite lift coil forces are therefore dependent upon the speed of the vehicle and were calculated by Davey (1995b) as :

$$F_y(100 \text{ mph}) = 589.77y + 0.808 \quad (4a)$$

$$F_y(200 \text{ mph}) = 644.4y + 0.7785 \quad (4b)$$

$$F_y(300 \text{ mph}) = 664.55y + 1.796 \quad (4c)$$

A plot of these relationships showing the variation of the composite lift coil force with displacement for various speeds is presented in Figure 7.

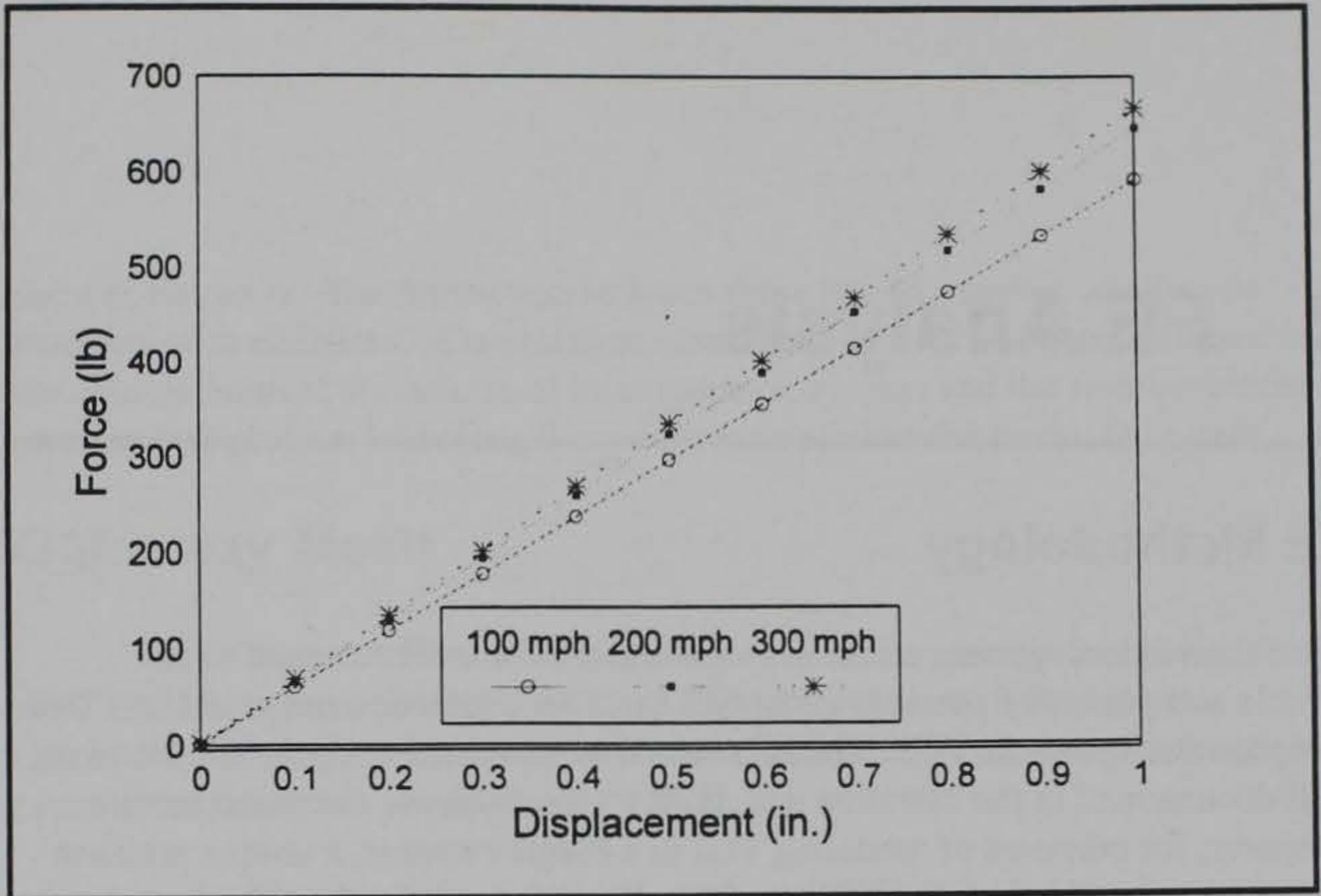


Figure 7. Composite coil lift force for various speeds

3 FE Analysis

FE Methodology

The FE methodology was utilized to simulate the dynamic response of the vehicle and guideway portions of the SCD and the interaction between these two components, known as VGI. The FE method of structural analysis in general is well documented in the literature and, thus, its theory is not discussed herein. However, for purposes of modeling VGI in a Maglev system, a unique problem arises in the application of the FE method. The FE mesh for the vehicle system (including its suspension) must be moved over the FE mesh for the guideway structure to simulate the vehicle's forward motion across the guideway. This was accomplished using interaction surfaces referred to as "slidelines" within the ABAQUS/Standard code (Hibbitt, Karlsson and Sorensen, Inc. 1994). The "slideline" elements available in the ABAQUS/Standard elements library are the cornerstone of the FE VGI methodology. These elements allow modeling of the interaction between deformable structures along sliding surfaces, where separation and/or sliding are of finite amplitude, and arbitrary rotation of the surfaces may arise. Slideline elements use a "master-slave" concept to enforce the contact constraints. The surface on which the slideline elements are placed is the "slave" surface. A specific set of nodes is then defined as the "master" surface. The slideline elements (or the slave surface) slide over the slideline (or master) surface. The nodes of the slideline elements are constrained not to penetrate into the master surface. Generally, the master surface is chosen as the surface of the stiffer body if the materials are different, or as the surface with the coarser mesh. The slave surface is defined by attaching slideline interface elements to the surface of one of the bodies in a predefined plane (that is assumed to intersect the surface orthogonally) and associating these elements with a set of defined slideline nodes in the same plane. Relative motion along the line of interaction can be arbitrarily large, but relative motions out of the plane containing the line of interaction are neglected, and so must be small compared to typical element sizes on the surface.

Based on the above description of slidelines, their usefulness for modeling VGI in a Maglev system can easily be seen. The guideway and the vehicle (including its complete suspension system) can be modeled to any desired degree of accuracy using finite elements. The suspension system of the vehicle(s) can be modeled with combinations of linear and nonlinear spring and

damper elements. The interaction between these two FE meshes can then be modeled with slidelines. The slideline elements (slave surfaces) are attached to the vehicle mesh at the bottom of its suspension system, and the slideline nodes (master surfaces) are laid along the guideway mesh like the tracks for a train.

Guideway Mesh

The FE mesh of the American Maglev guideway is depicted in Figure 8. All FE modeling was accomplished in 2-D, since sufficient 3-D response characteristics (such as guideway curvatures, and vehicle roll, and yaw inertial capabilities) were not available on the SCD.

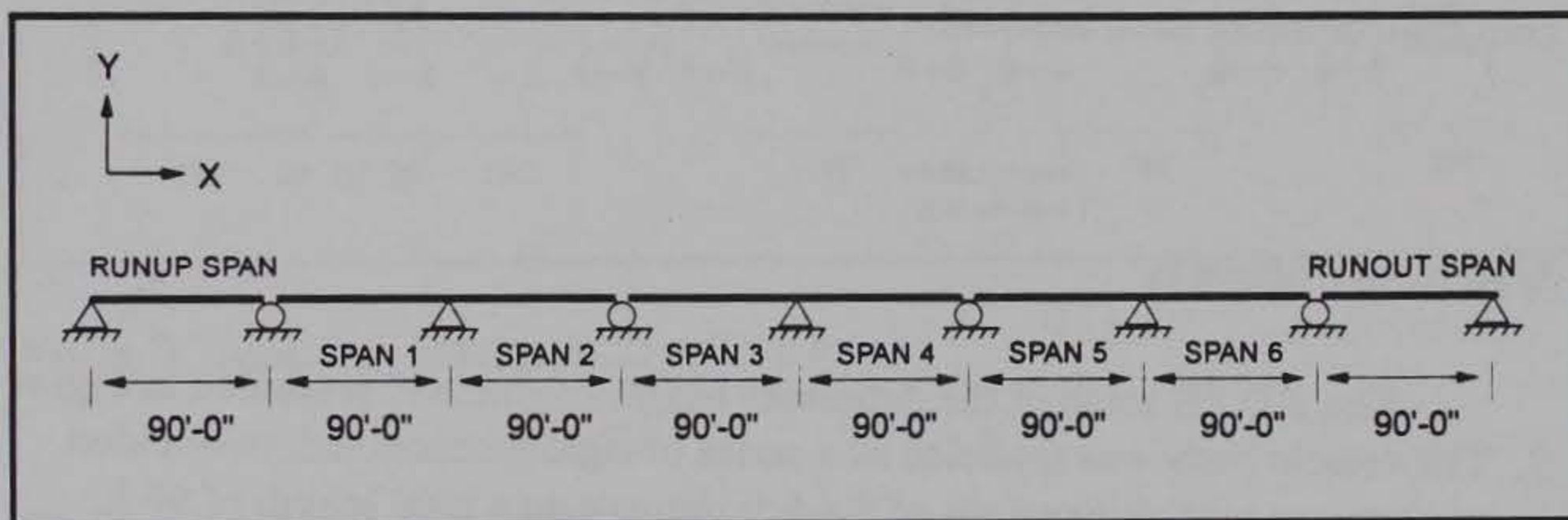


Figure 8. American Maglev SCD guideway mesh

In order to study the vehicular response over a significant length of guideway, a series of three two-span continuous sections of guideway were modeled, i.e., a total of six spans at 90 ft each with continuous spans at every other support. Notice also in Figure 8 that a "runup" and a "runout" span were defined at each end of the guideway mesh. These portions were of the same length as the vehicle (90 ft) and provided a starting point (prior to entering the actual spans under consideration) and an ending point for the vehicle in order to get the vehicle completely off the actual spans. The spans were made very stiff not to induce initial displacements into the vehicle prior to entering the critical spans.

The actual guideway spans were modeled using two-noded rectangular beam elements, each 20 in. long. They represented the composite guideway section formed by two PSC beams and a CIP slab (as discussed previously). They had a width and height of 96- and 63 in., respectively. These dimensions were chosen to provide a transformed moment of inertia of $1,999,784 \text{ in.}^4$, with a

corresponding mass density of 9.9×10^{-5} lb-sec²/in⁴. The mass of the intermediate diaphragms was neglected. A linear-elastic material model was used to represent the concrete with an elastic modulus of 4,888 ksi.

While the actual guideway design is prestressed, no prestressing or reinforcing was included in the FE model since these details were not available, and calculation of internal bending stresses was not desired from these analyses. Conversations with the American Maglev designers indicated that the prestressing would be used to effectively remove dead-load deflections. No mention was made of using upward camber to benefit ride quality, as has been done in the past with other Maglev systems (Lever 1993). Therefore, the prestressing effect was simulated in the FE model through application of an upward uniform load equal to 2.78 k/ft (equal to the dead load of the superstructure) which eliminated dead-load deflections and effectively provided zero camber under dead load only.

Vehicle Mesh

The 2-D FE mesh of the American Maglev vehicle is presented in Figure 9. The vehicle body was modeled as a series of rigidly connected, two-noded beam elements with dimensions of 8 × 8 ft throughout a total length of 90 ft. Since a mass distribution was not specified in the references, the total weight of the vehicle (40 tons) was distributed uniformly over its length. This corresponded to a mass density of 2.1×10^{-5} lb-sec²/in⁴. Vehicle flexibility was also undefined. Since this was considered to have little effect on the total dynamic response of the system, a very stiff modulus of elasticity equal to 30,000 ksi was used to keep this mode of response at a minimum.

The suspension for the vehicle was modeled as a series of overlapping spring elements connected to the vehicle beam elements at their top end and to the slideline elements at their bottom end. As seen in Figure 9, the springs were located along the length of the vehicle at each C set magnet pair location, as previously shown in Figure 2. Two overlapping spring elements were used to represent each C set, which experiences a combined lift force from the composite lift coil (with a linear force variation) and the active lift coil (with a nonlinear force variation). A linear spring was used to represent the lift from the composite lift coil, while a nonlinear spring was used to represent that one associated with the active lift coil. The springs were given an unrealistically long length of 4 ft to ensure a sufficient gap allowance for settlement and total dynamic response.

As shown in Figure 7 and Equations 4a through c, the force-displacement relationship for the composite lift coil is linear and varies with the vehicle's forward velocity. The slope of the lines in this figure, of the first derivative of Equations 4 a through c, was used to define the spring constants, k , for the linear springs at specific vehicle velocities. Since the FE model is 2-D, the spring constant values were multiplied by 2 to appropriately represent the right and left side of the C sets at each location along the length of the vehicle.

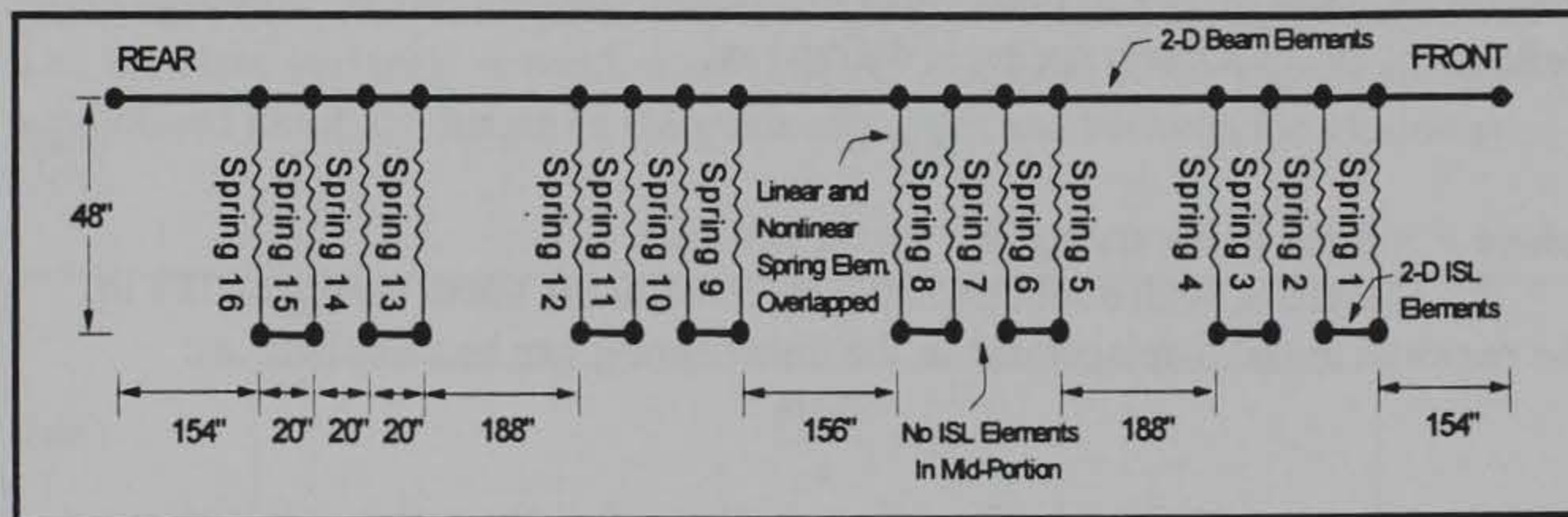


Figure 9. American Maglev SCD vehicle mesh

The resulting spring constants were as follows:

$$k_y(100 \text{ mph}) = 589.77(2) = 1179.54 \text{ lb/in.} \quad (5a)$$

$$k_y(200 \text{ mph}) = 644.40(2) = 1288.80 \text{ lb/in.} \quad (5b)$$

$$k_y(300 \text{ mph}) = 664.55(2) = 1329.10 \text{ lb/in.} \quad (5c)$$

The force-displacement function for the active lift coil was previously shown in Equation 1 and depicted graphically in Figure 4. This function was used to define the behavior of the nonlinear springs of the vehicle mesh. The properties of the nonlinear springs were defined in a numerical form inside the ABAQUS/Standard input file (Hibbitt, Karlsson and Sorensen, Inc. 1994), which is included in Appendix A. Careful review of this segment of the input file will reveal that the displacement magnitudes do not correspond to those shown in Figure 4. The displacement values are actually offset by 3.5 in., and the explanation for this is presented in the following paragraph.

As discussed previously, American Maglev chose an initial offset (overburden) of 1.5 in. on these coils to prevent instabilities in the system. From the curve shown in Figure 4, it can be observed that this offset will correspond to a lift force of approximately 2,308 lb. Because this is a 2-D FE model, the

nonlinear spring force at each C set location will need to be equal to $2,308 \times 2 = 4,616$ lb to properly simulate the total lift force. This is the force required by the nonlinear springs at the beginning of each dynamic FE analysis. The total weight of the vehicle is 80,000 lb and, assuming the weight is evenly distributed between all 16 spring sets, each spring set (i.e., overlapping linear and nonlinear springs) will support an approximate weight equal to 5,000 lb (calculated as: $80,000 \text{ lb} / 16 \text{ spring sets} = 5,000 \text{ lb}$). If the nonlinear springs support 4,616 lb of the total 5,000 lb, then the overlapping linear springs must supplement the supporting force by 384 lb (calculated as: $5,000 - 4,616 = 384 \text{ lb}$). The deflection, Δ , of a linear spring is defined as:

$$\Delta = \frac{F}{k} \quad (6a)$$

where F = force in the spring, k = spring constant.

Therefore, with a required starting force in the linear spring of 384 lb, the required initial displacement in the linear spring can be calculated as:

$$\Delta = \frac{384/b}{k} \quad (6b)$$

Using the k values defined by Equations 5a through c, the required initial displacements were thus equal to 0.326-, 0.298-, and 0.289 in. for 100-, 200-, and 300 mph, respectively. Thus, it can be concluded from this discussion that two specific initial conditions had to exist at the beginning of the dynamic FE analysis to accurately represent the actual design of the vehicle: a starting force per nonlinear spring equal to 4,616 lb, and an initial displacement of approximately 0.30 in. for each linear spring to get the required supplement force of 384 lb. This supplemental force was applied by artificially offsetting the displacement magnitudes (not differentials) of the nonlinear force-displacement relationship to the point that a downward displacement of 0.30 in. corresponded to a force of 4,616 lb in the nonlinear spring.

In order to verify that the nonlinear springs were properly defined in the FE mesh, a simplified mesh was first analyzed. It consisted of a single lumped mass element suspended on a single nonlinear spring with the same characteristics as those used in the actual vehicle mesh. The lumped mass was given a weight of 5,000 lb, which corresponds to 1/16th of the total vehicle weight, since there are 16 springs on the actual vehicle model. A dynamic analysis was performed, with a time increment equal to 0.01 sec for a total time period of 0.5 sec. Figure 10 shows the resulting vertical displacement history of the mass as it settled on the spring. It can be observed from this figure that the vertical displacement followed a pattern similar to that followed by the curve shown in Figure 4. This indicates that the behavior of the nonlinear spring element was properly defined.

Slidelines

As described in a previous section, the *SLIDELINE option in the ABAQUS/Standard code (Hibbitt, Karlsson and Sorensen, Inc. 1994) was used to provide the sliding interaction between the vehicle and the guideway mesh. The slideline elements were attached between adjacent nodes corresponding to the bottom ends of the vehicle spring elements. Their nodal connectivity was set as a hinge-type connection to allow independent vertical responses at each of the spring elements, while still providing the sliding interaction along the guideway (i.e., the slave surface). A continuous slideline surface (i.e., the master surface) was defined along the length of the guideway mesh and between the guideway nodes.

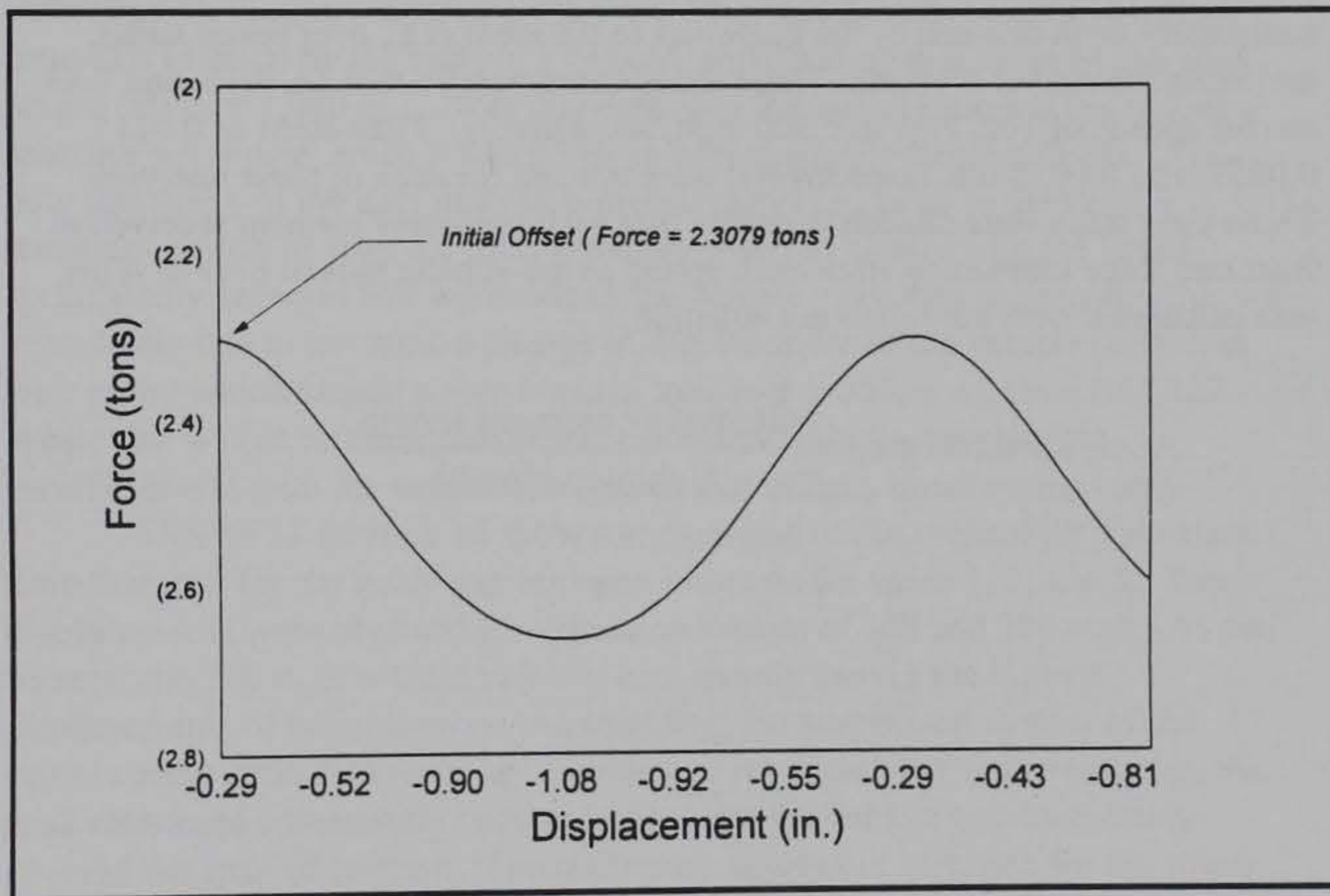


Figure 10. Variation of the active lift force with displacement

Dynamic Analysis

The ABAQUS/Standard FE code (Hibbitt, Karlsson and Sorensen, Inc. 1994) was used for the dynamic analysis of the American Maglev mesh. A typical analysis input file is included in Appendix A. The vehicle was effectively moved across the guideway mesh at a constant forward velocity by applying a velocity boundary condition to all of the nodes associated with the vehicle mesh. Analyses were made for vehicle velocities of 100-, 200-, and 300 mph. Separate analyses were also made using only the linear spring suspension (i.e., the composite coil lift) for the same velocities. For these analyses, the linear spring constants in Equations 5 a through c were multiplied by a factor equal to 12.3115, according to Davey (1994).

Each FE analysis was run for the total time required to move the vehicle completely from one end of the guideway to the other (i.e., over seven spans, including the runout section). These times corresponded to 4.36, 2.16, and 1.43 sec for speeds of 100, 200, and 300 mph, respectively. Time-steps of 0.0115, 0.0057, and 0.0038 sec, respectively, were utilized for each of these analyses. These time steps were chosen to ensure that each guideway element received at least one force interaction from each spring as the vehicle moved over it. This was calculated with the following equation:

$$\text{Analysis time - step} = \frac{\text{Guideway element length}}{\text{Vehicle velocity}} \quad (7)$$

4 Analytical Results

The results obtained from the dynamic analyses are presented in Figures 11 through 30. Each analysis was performed for two different scenarios: the vehicle when supported only on its composite lift coil suspension system (referred to herein as "Linear Springs Only"), and with the vehicle supported by both the composite lift and active lift coil systems (referred to herein as "Both Springs"). All the results presented herein were nondimensionalized according to the position of the front of the vehicle (i.e., head position) with respect to each individual 90-ft span length of guideway. This was done by multiplying the time-axis (x-axis) by the vehicle's velocity and dividing this value by the span length (90 ft or 1,080 in.). Note that data after the vehicle entered the runout span are not shown, since it was given an unrealistically large stiffness. Also note that many of the data plots stop prematurely (i.e., prior to the vehicle reaching the end of span 6). This situation occurred mostly with the linear-springs-only scenario and worsened as the vehicle velocities increased. This was most likely due to too rapid a change in displacement of the vehicle (shown in later plots) which caused a convergence tolerance problem within ABAQUS. While this was an internal convergence problem, it indicates possible insufficiencies with the suspension system that utilizes linear springs only.

Figures 11 through 16 show a comparison of the vertical displacement time-histories for the guideway midspan locations for spans 1, 2, and 5. These displacements were obtained for vehicle velocities of 100 and 300 mph. As can be seen, the 300 mph vehicle velocity consistently caused the highest displacements of the guideway. As expected, the suspension system of the vehicle made little difference as to guideway response. For both velocities, the peak responses consistently occurred only after the vehicle had completely covered the span of concern. The maximum downward response for the linear springs only system was 0.17 in. on span 2 and for the system with both springs, was 0.13 in. on span 2. For spans of 90 ft (or 1,080 in.), these correspond to very high span-deflection ratios of $L/6,400$ and $L/8,300$, respectively. For a static midspan deflection of 0.095 in. (two-span beam with a uniformly applied vehicle load on one span), these correspond to dynamic load factors (i.e., ratio of dynamic to static deflection) for the guideway of 1.79 and 1.37, respectively. All of these values are well within previously established design criteria for other U.S. Maglev systems (Lever 1993).

The vertical displacements of the vehicle as it traversed the guideway spans are presented in Figures 17 through 20. The displacements shown are those of the vehicle nodes at the attachment points for Spring 1 (denoted as "Vehicle's Front") and Spring 16 (denoted as "Vehicle's Rear"). These locations are shown in Figure 9. From these plots it can be seen that the 300-mph velocity caused the greatest deflections for the case of the vehicle on linear springs only. However, when both suspensions were included, the exact opposite was true; the 100-mph velocity caused the highest response and the 300-mph velocity caused the lowest. Note that with both springs and at 300 mph, the vehicle displacement continued to increase with each successive span. This result shows the importance of multiple-span analyses as conducted herein and indicates the potential need for damping of the vehicle's suspension system.

The vertical accelerations corresponding to the same locations as the above displacements are shown in Figures 21 through 24. For the case of the linear springs only, the 300-mph velocity produced considerably higher accelerations in the 0.9-g range as compared to values less than 0.1 g for the 100-mph velocity. In addition, the increasing trend of the 300-mph curve indicates that accelerations over successive spans could be even greater. The accelerations for the vehicle with both springs were much lower, with the worst accelerations of approximately 0.12 g occurring at the 200-mph speed. The frequency of all of these accelerations was in the 1- to 5-Hz range. While these data show that the addition of the active suspension made a substantial improvement to the vehicular ride quality, the accelerations were still somewhat high compared to those for other SCD's as studied by Lever (1993). They showed that for accelerations in the 1- to 5-Hz range (as with the data herein), the ISO 1-hour reduced-comfort level is between 0.05 and 0.1 g. The accelerations calculated herein were at or above these limits.

Figures 25 and 26 show the variation in the nonlinear spring forces for the front and the rear part of the vehicle as it traveled through the guideway. As desired, the force in each spring started at 4,616 lb to represent the 1.5-in. offset in the nonlinear springs. Throughout the guideway traversal, the force variations stayed within a 200-lb range (or 100-lb per C set) for the 300-mph vehicle speed. The variations were as much as 450 lb (or 225-lb per C set) for the 100-mph speed. These variations were all well within the design force overburden or safety margin (see previous discussion of the suspension system) on these springs of 491-lb per C set.

Figures 27 through 30 show the change in length associated with the front and rear springs, which is representative of the vertical gap variation between the vehicle and the guideway throughout the vehicle traversal. Because of its null-flux type of suspension system, this is not as important for this system. The horizontal gap variation would be more important, but since this was only a 2-D analysis, these data of course were not obtained.

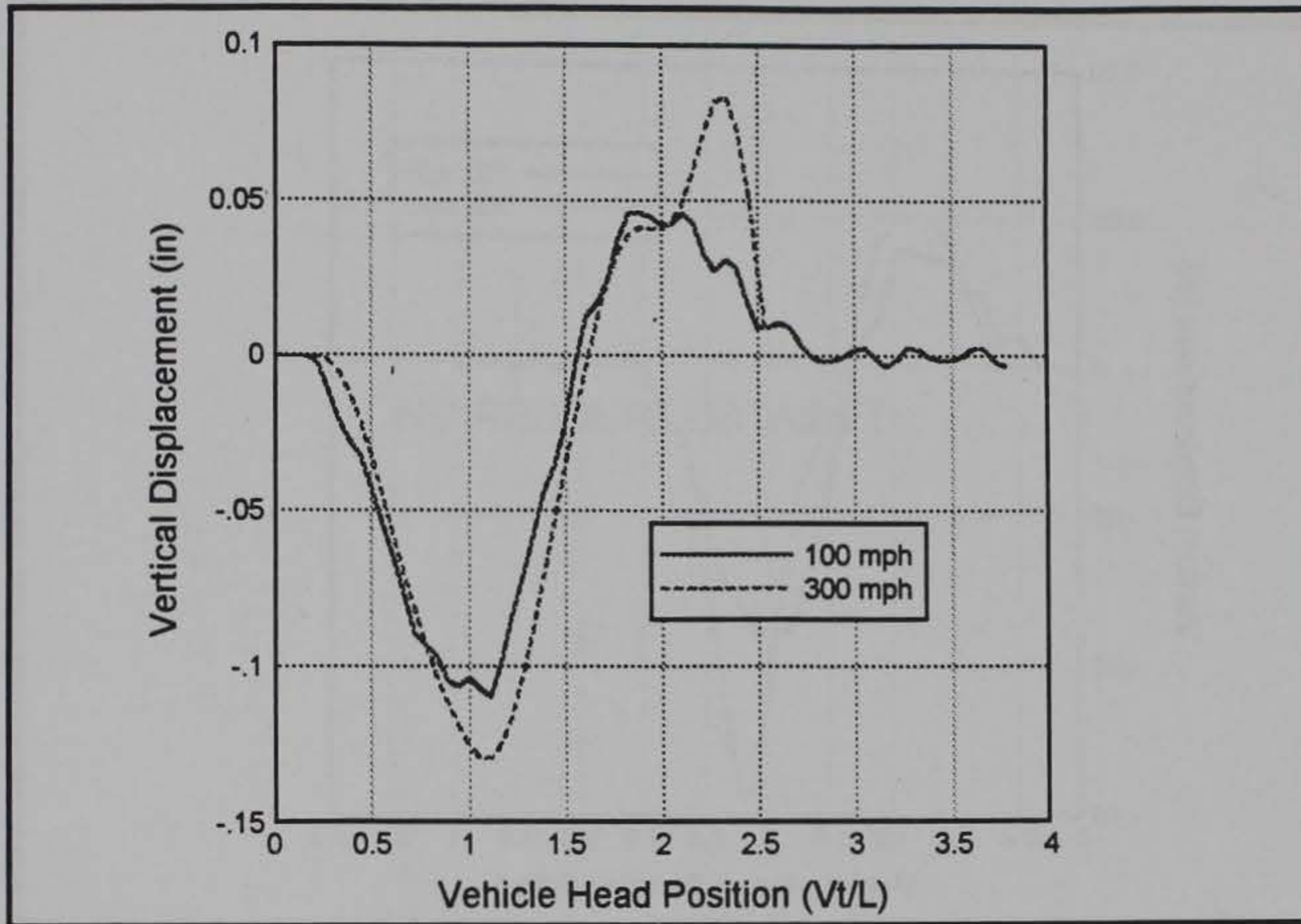


Figure 11. Vertical displacement of midspan 1 (linear spring only)

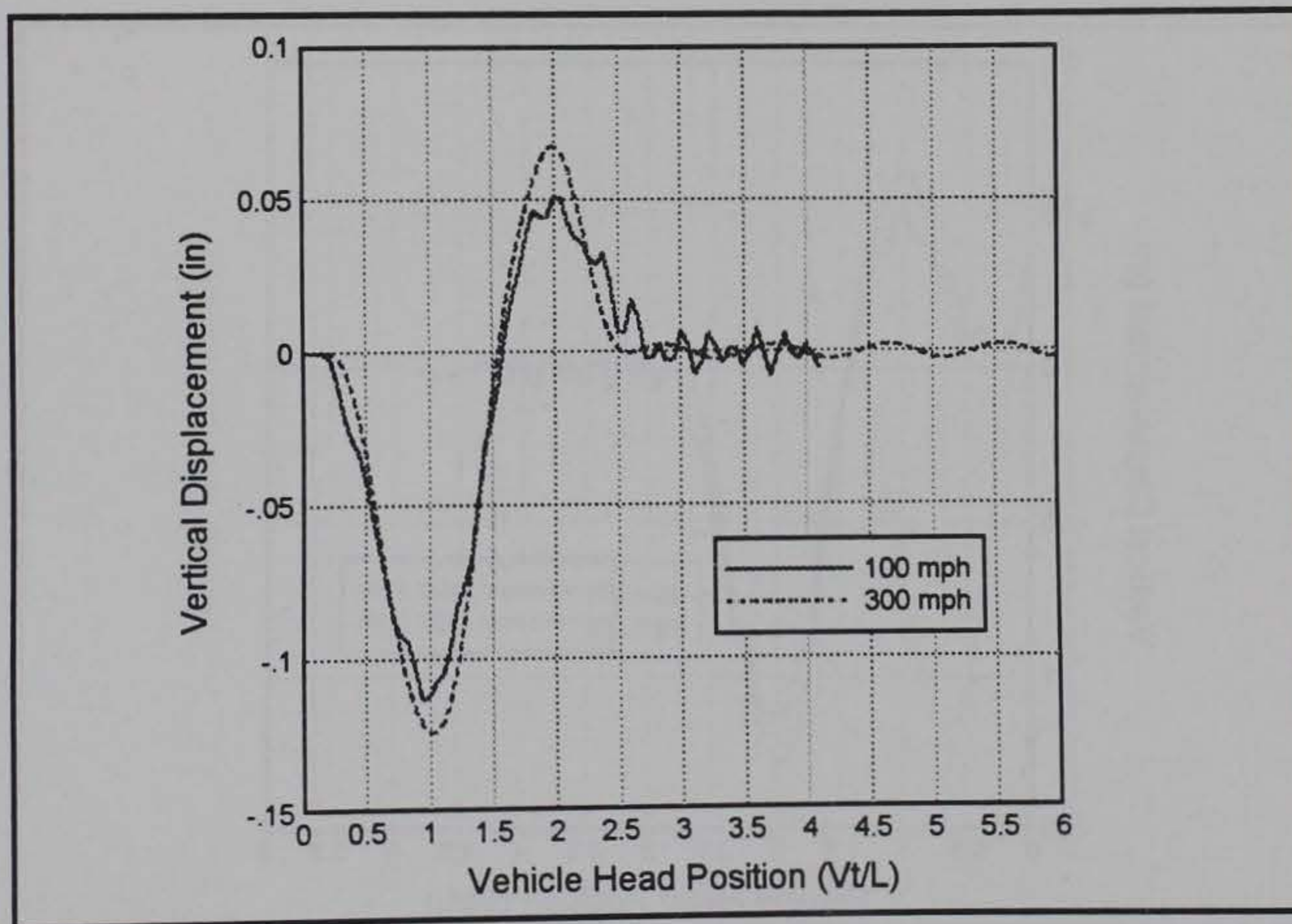


Figure 12. Vertical displacement of midspan 1 (both springs)

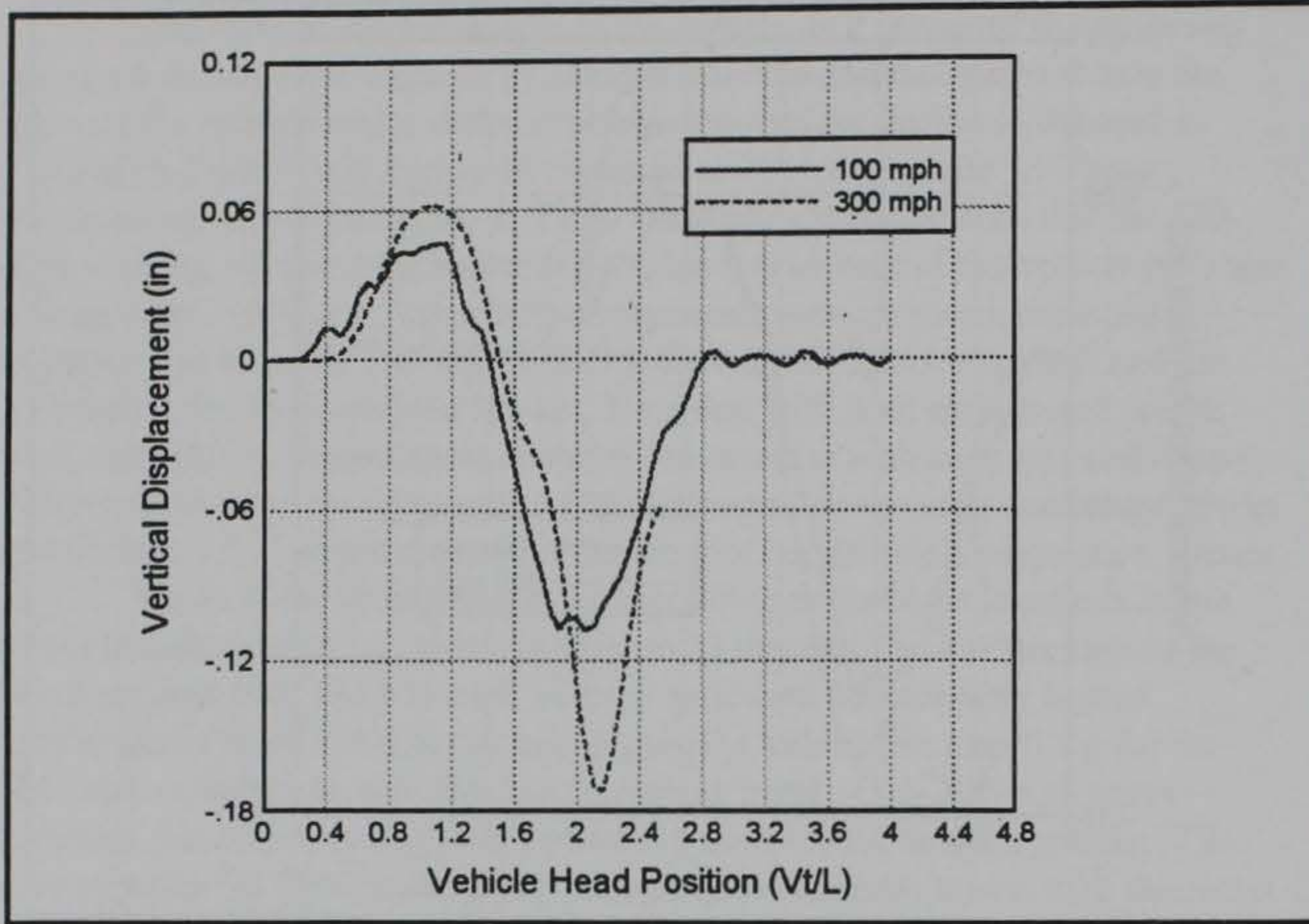


Figure 13. Vertical displacement of midspan 2 (linear spring only)

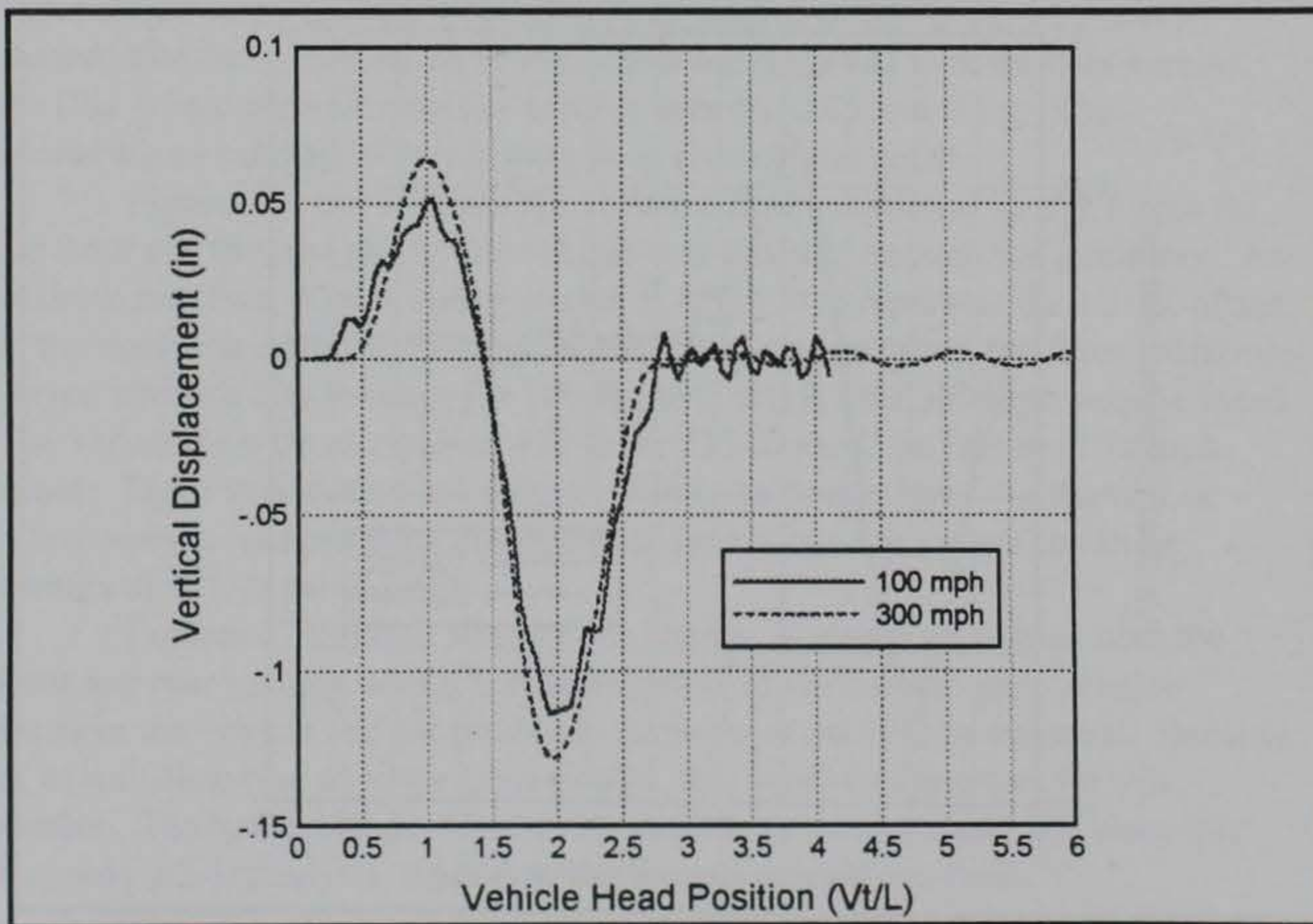


Figure 14. Vertical displacement of midspan 2 (both springs)

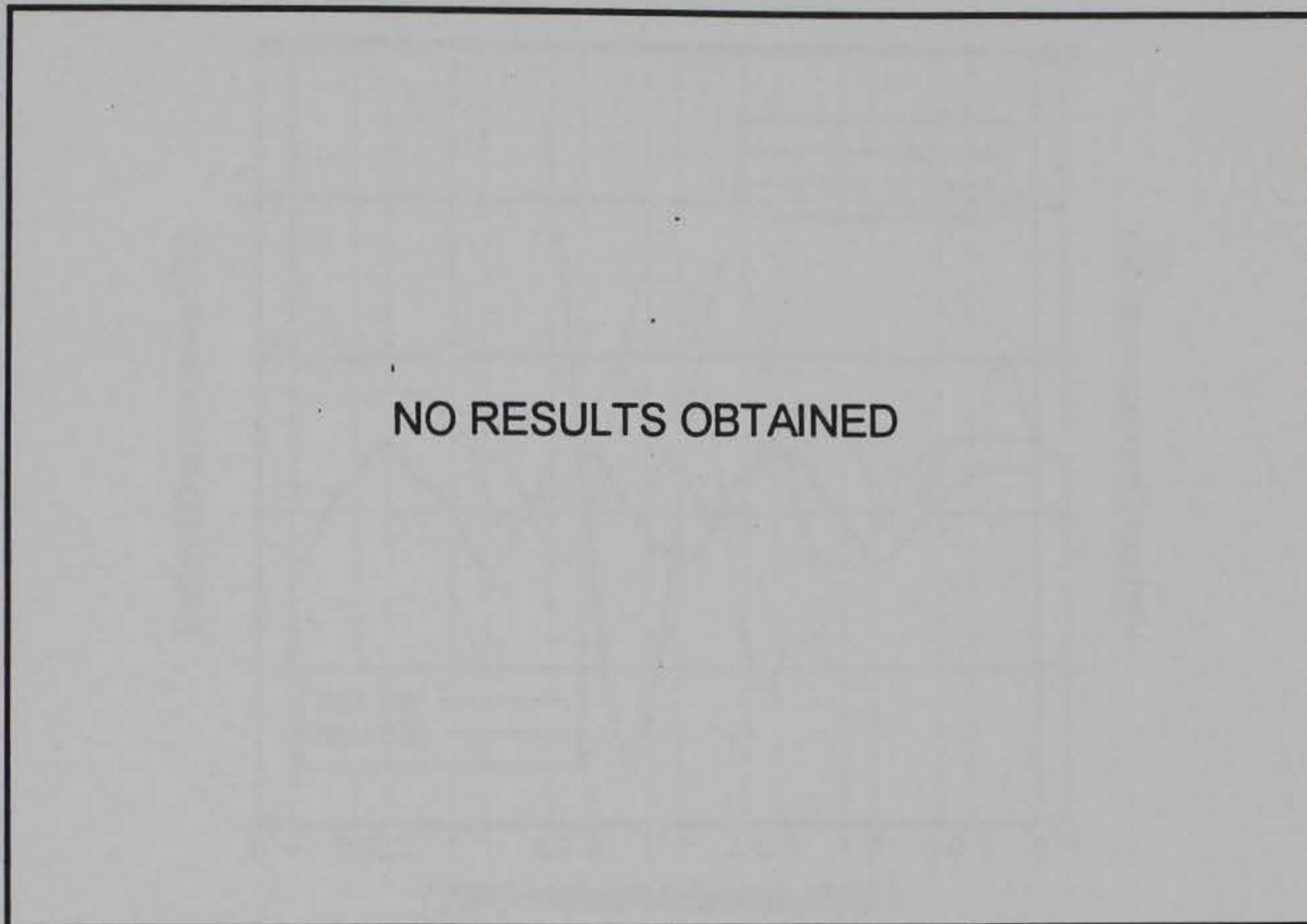


Figure 15. Vertical displacement of midspan 5 (linear spring only)

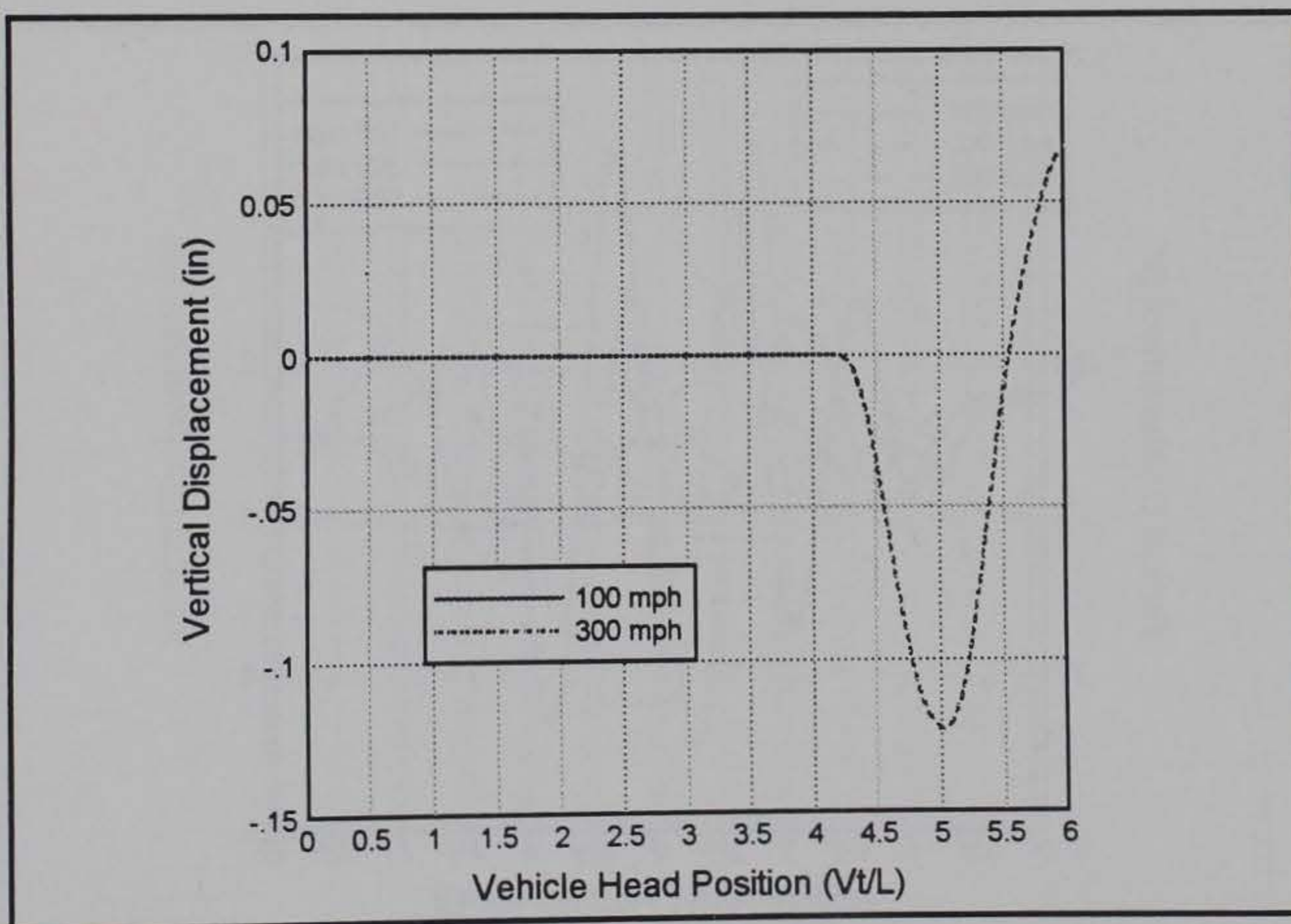


Figure 16. Vertical displacement of midspan 5 (both springs)

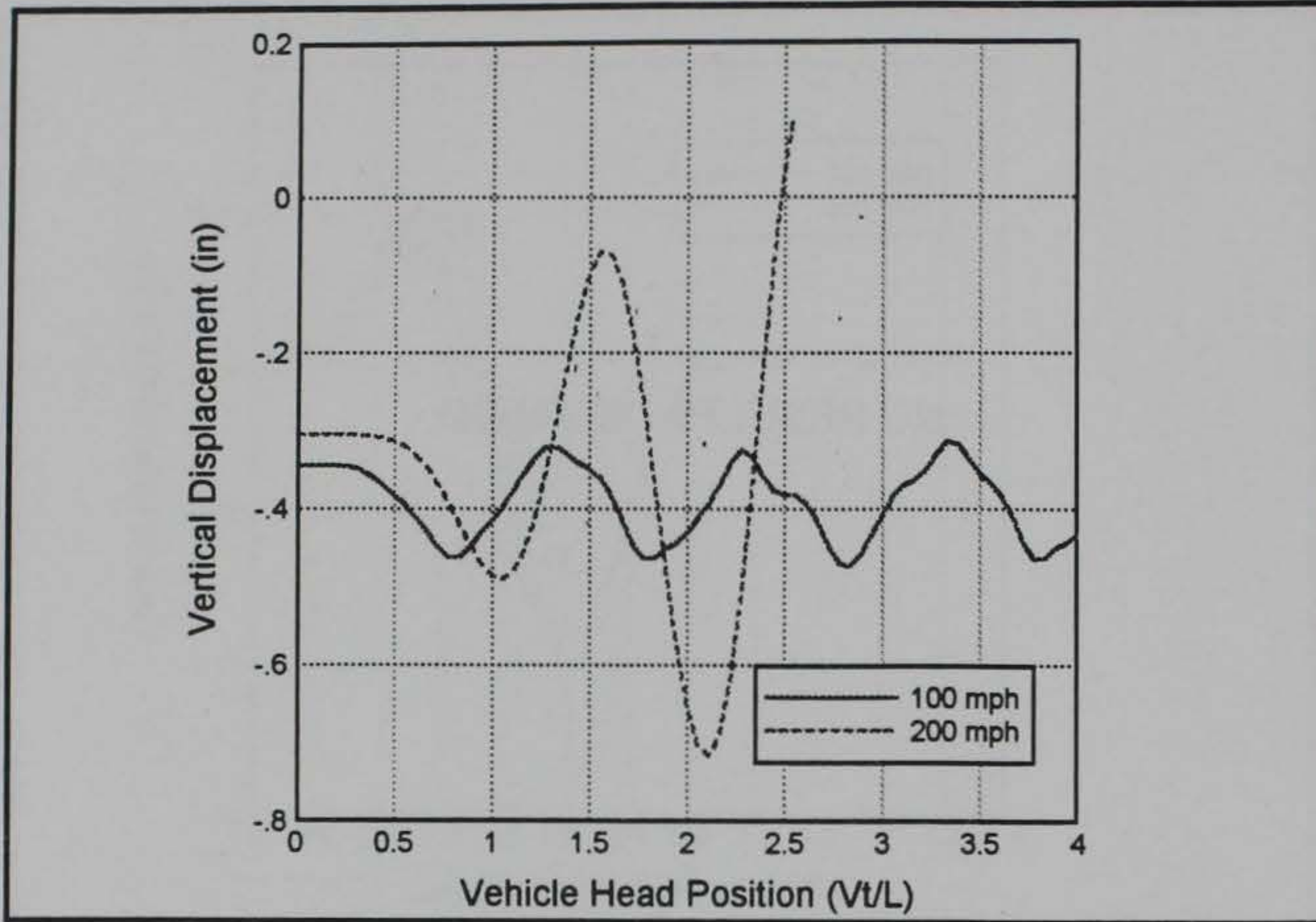


Figure 17. Vertical displacement of vehicle's front (linear spring only)

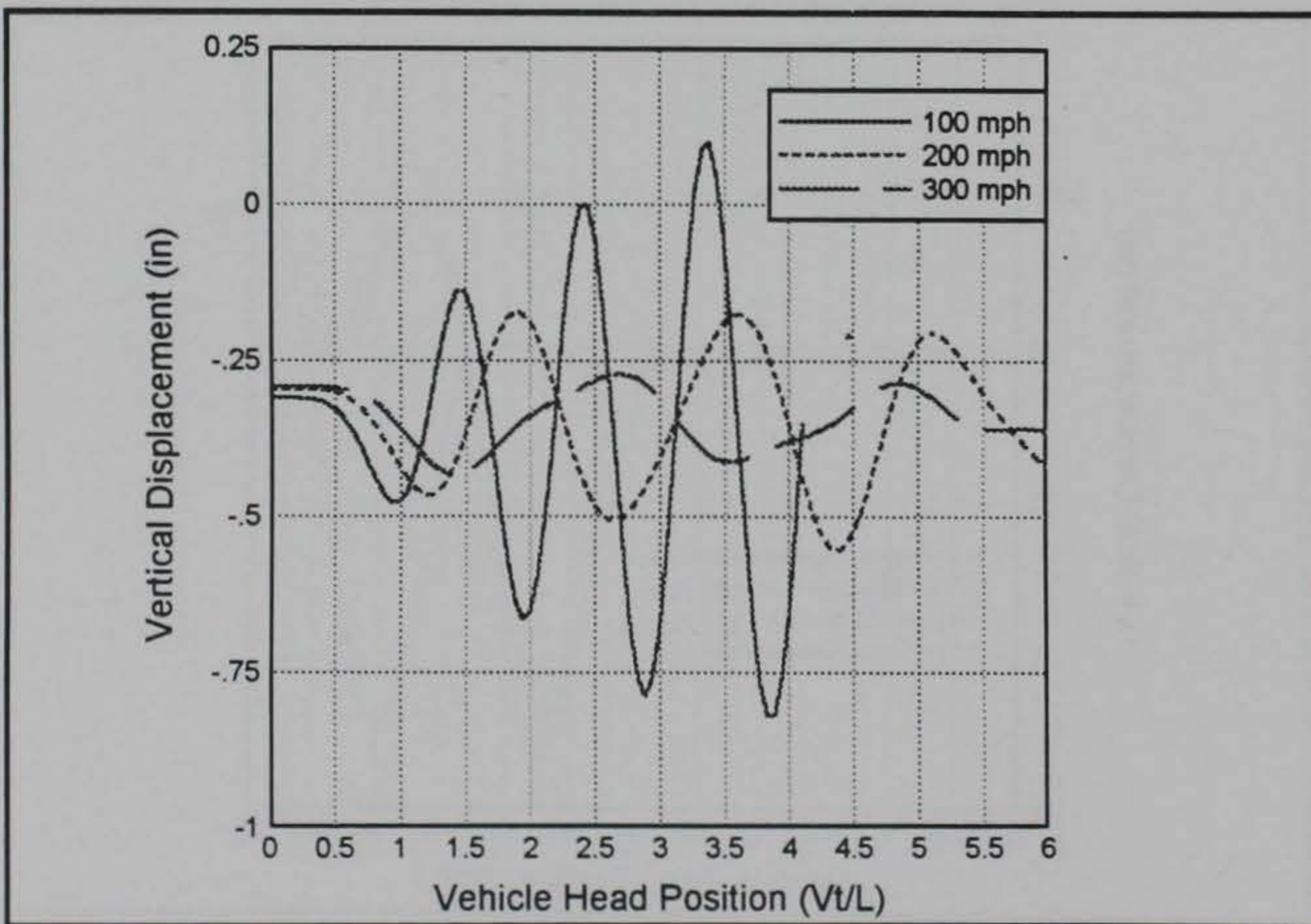


Figure 18. Vertical displacement of vehicle's front (both springs)

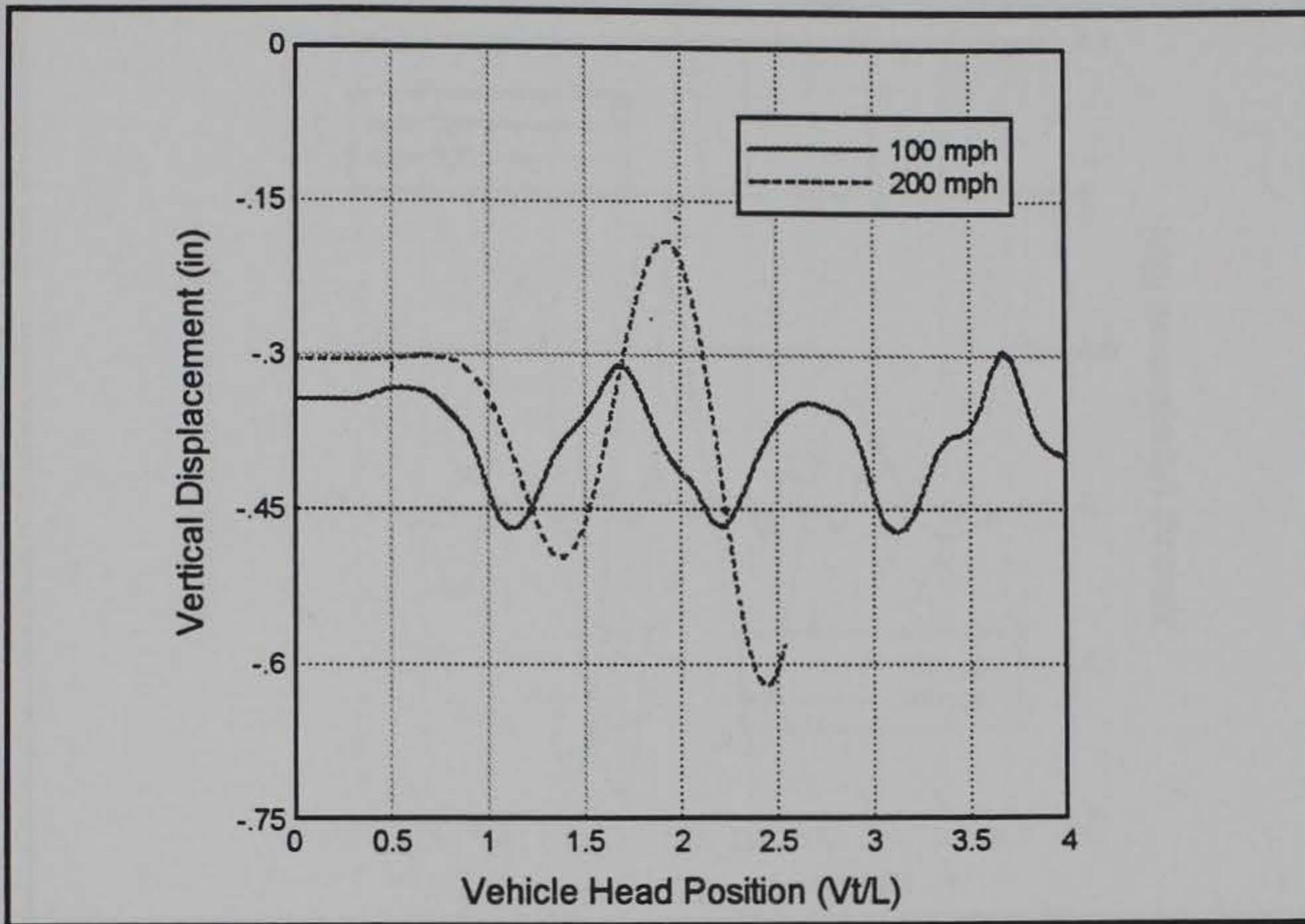


Figure 19. Vertical displacement of vehicle's rear (linear spring only)

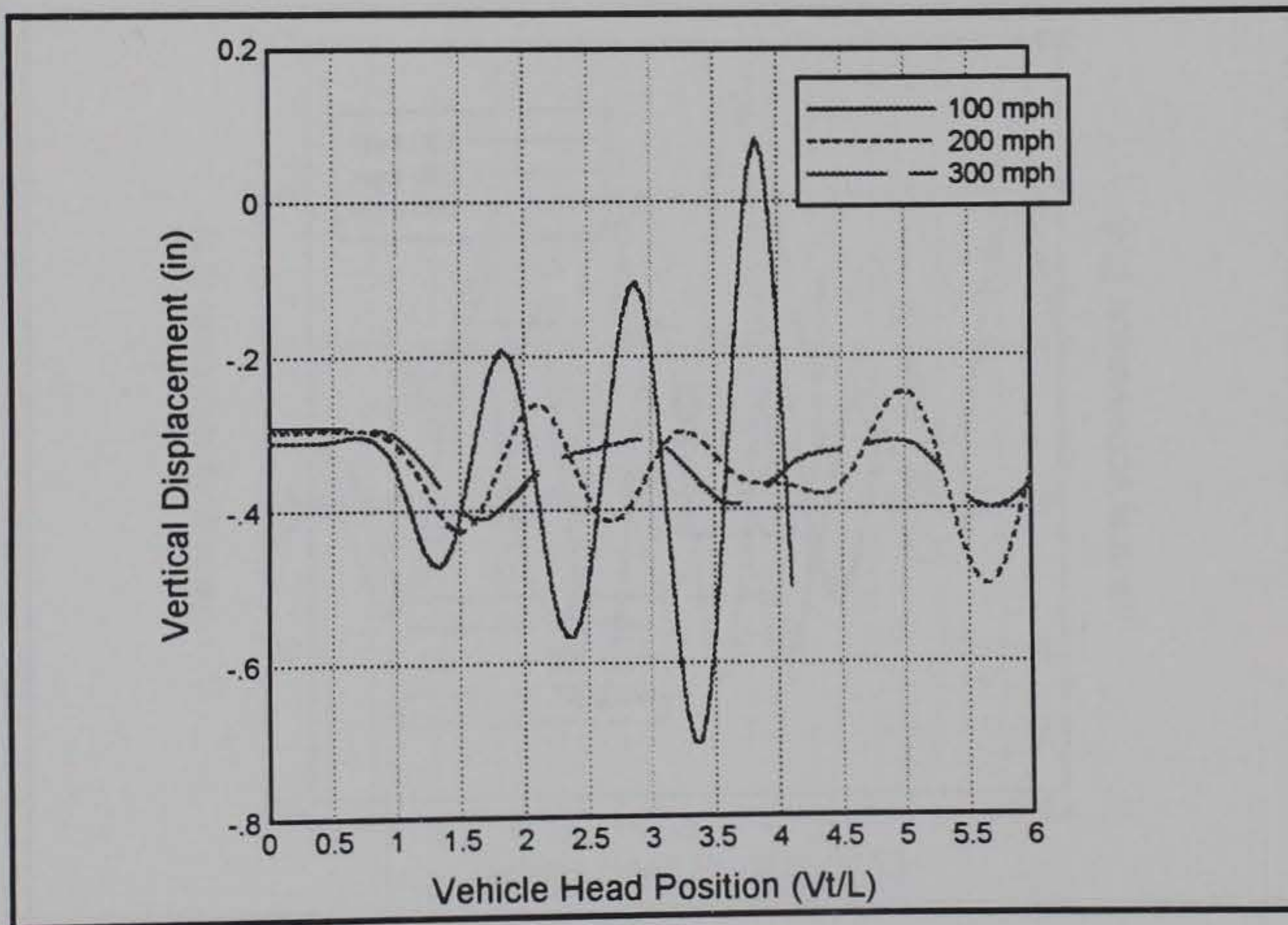


Figure 20. Vertical displacement of vehicle's rear (both springs)

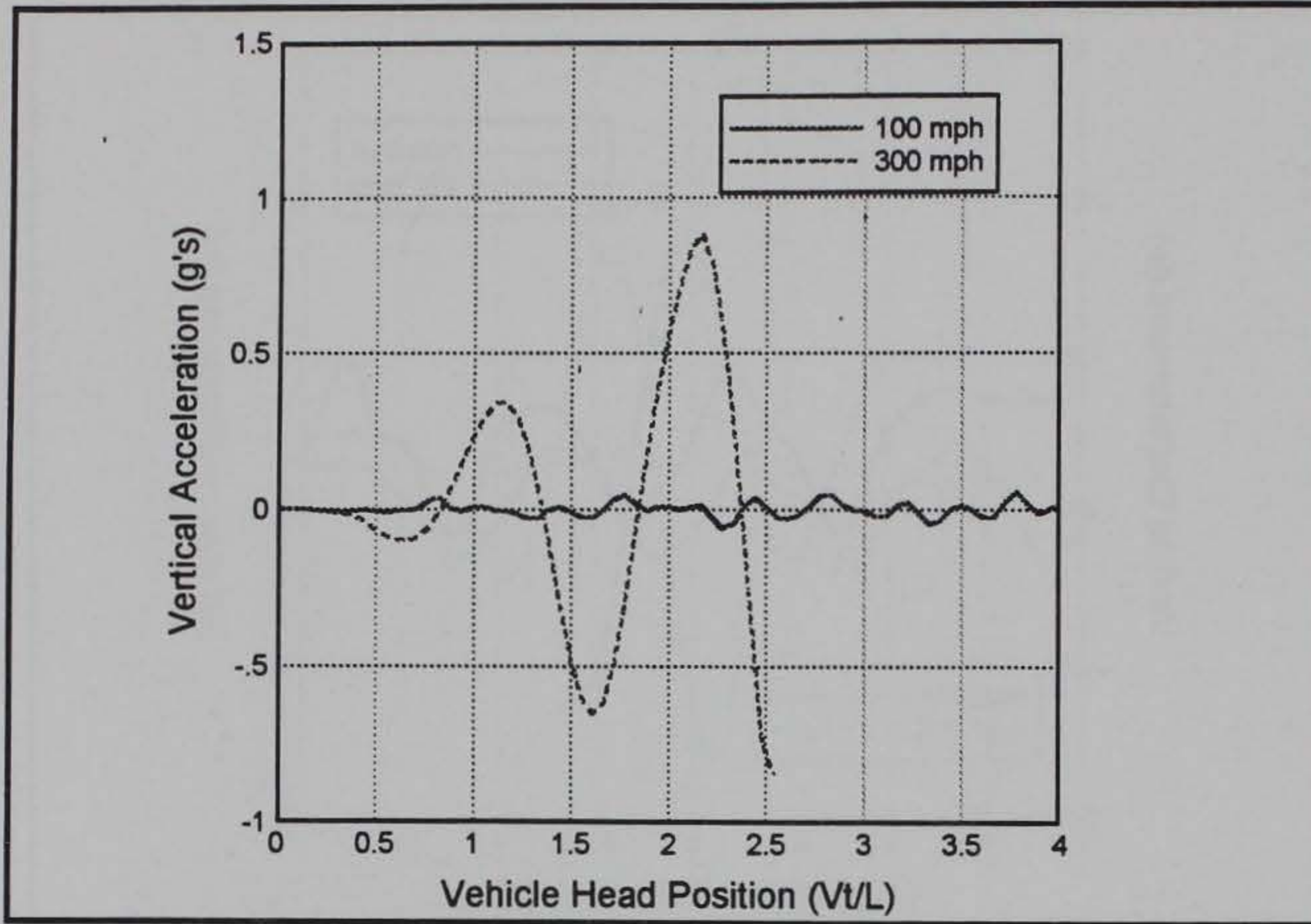


Figure 21. Vertical acceleration of vehicle's front (linear spring only)

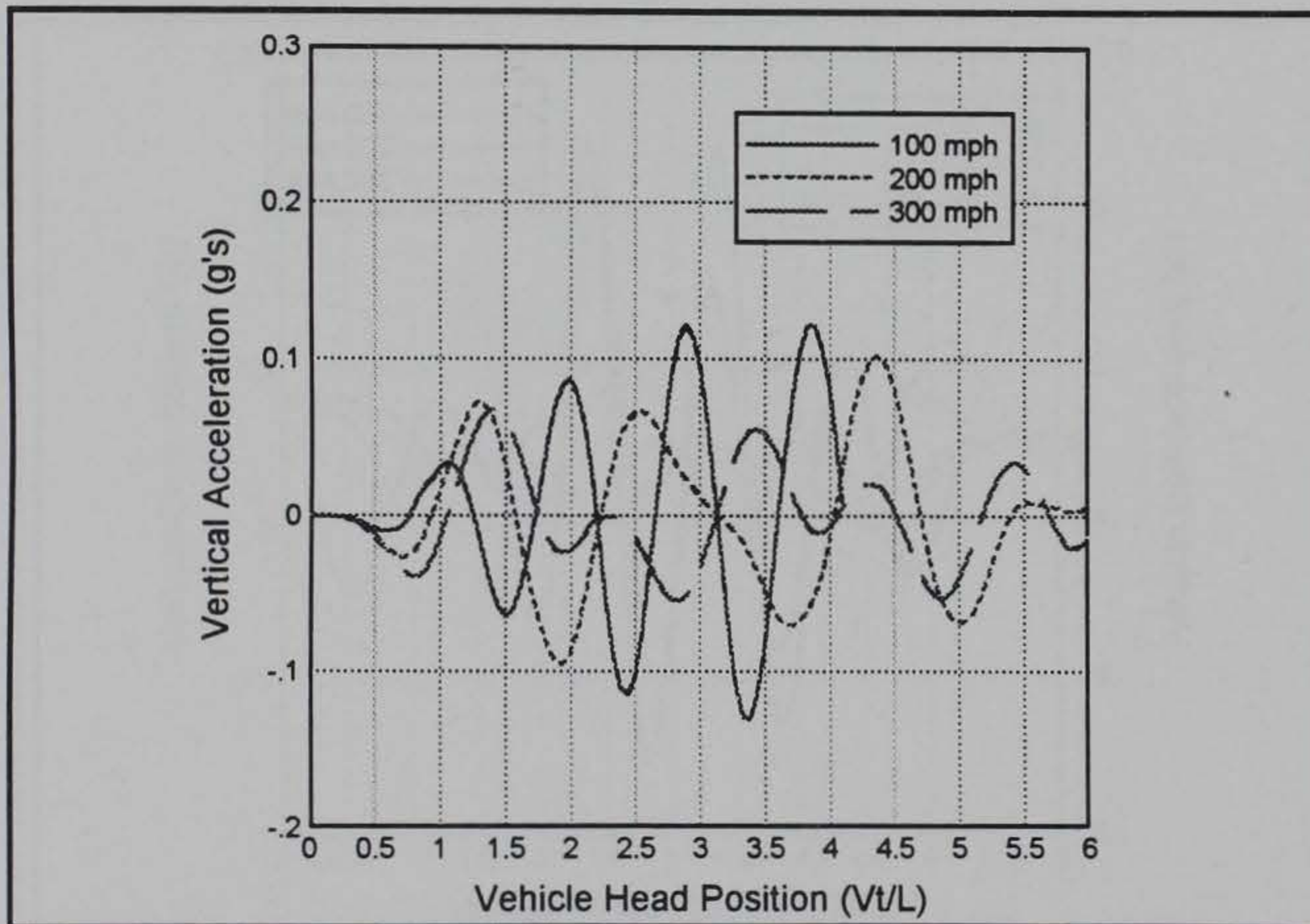


Figure 22. Vertical acceleration of vehicle's front (both springs)

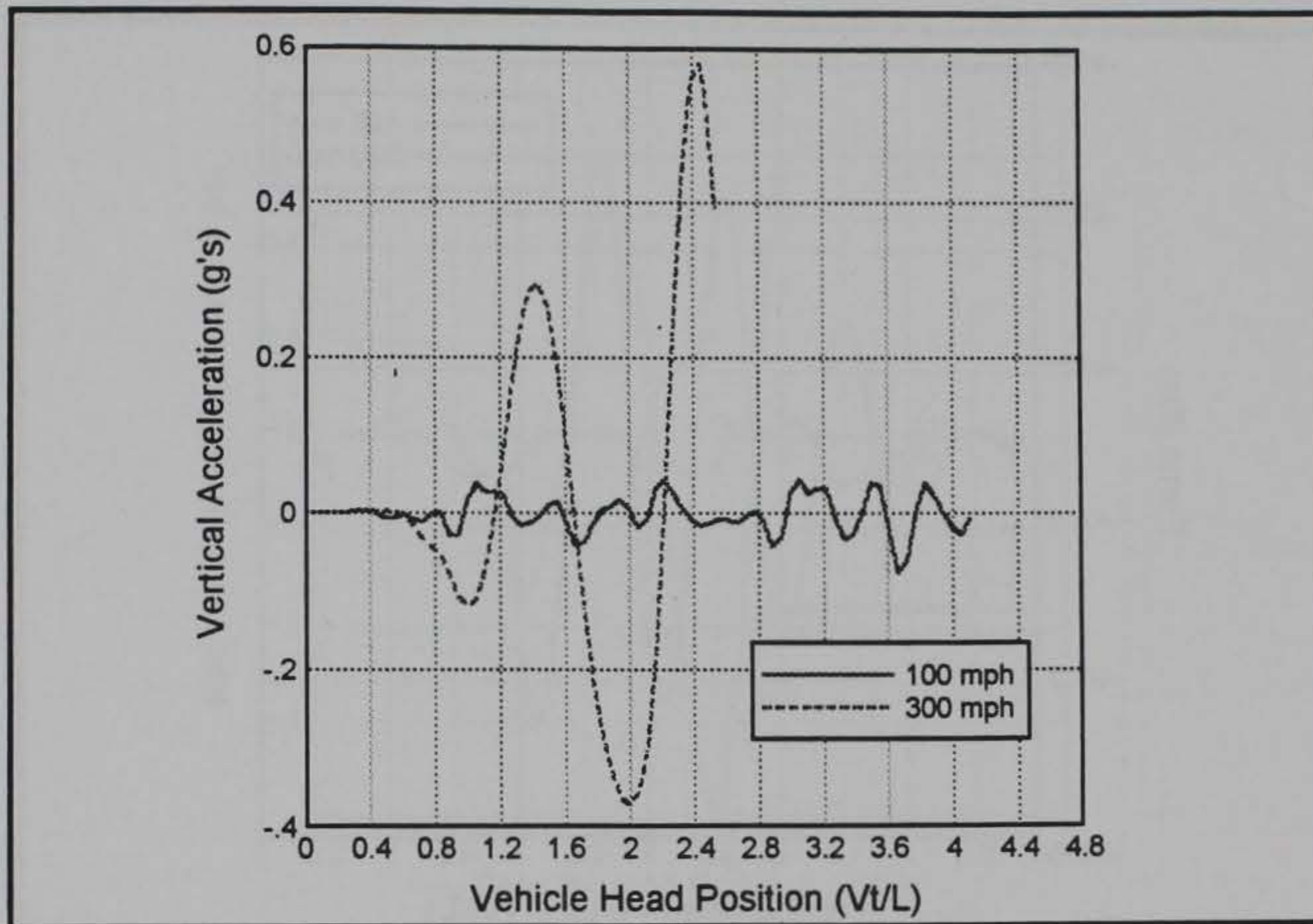


Figure 23. Vertical acceleration of vehicle's rear (linear spring only)

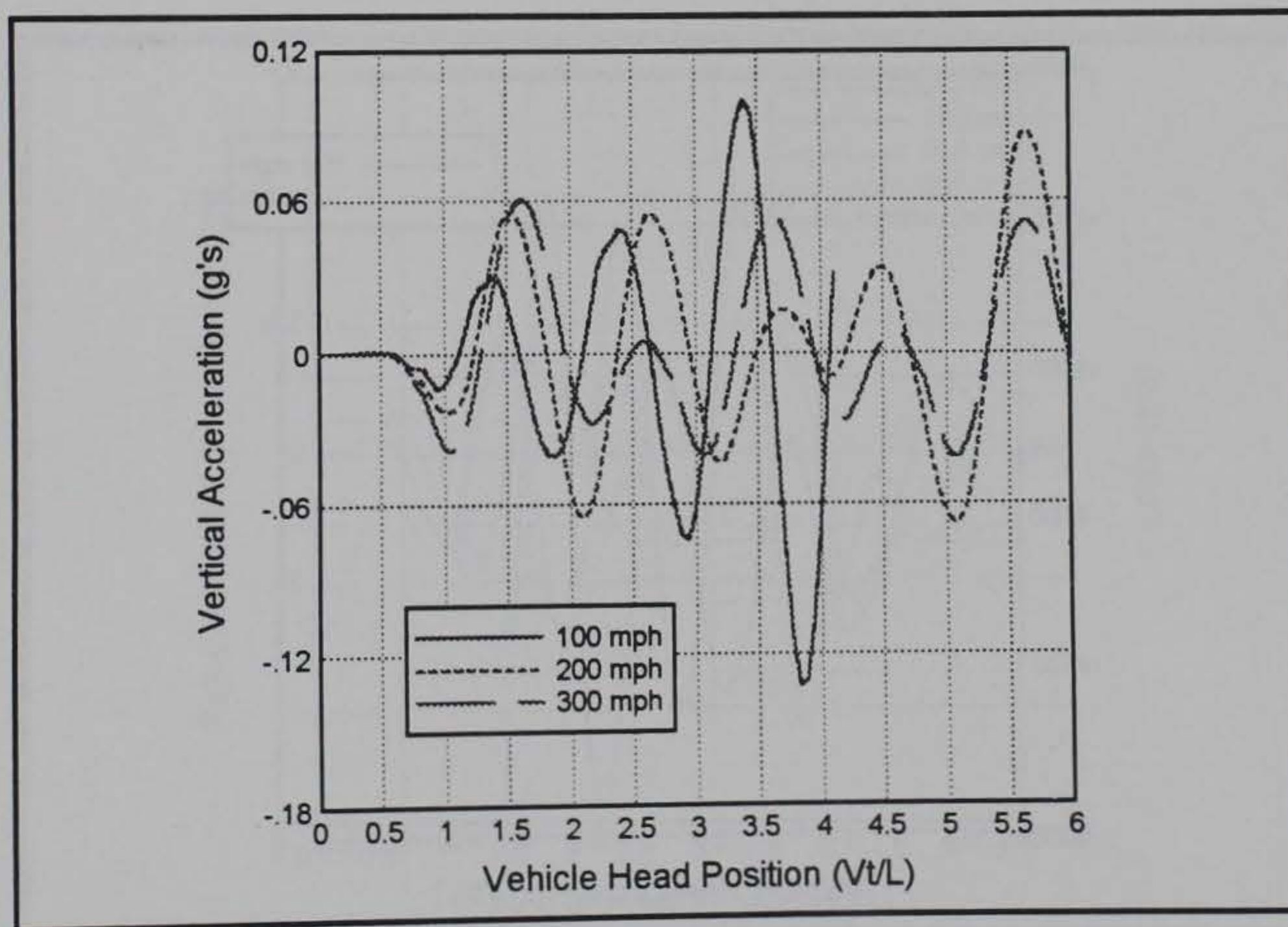


Figure 24. Vertical acceleration of vehicle's rear (both springs)

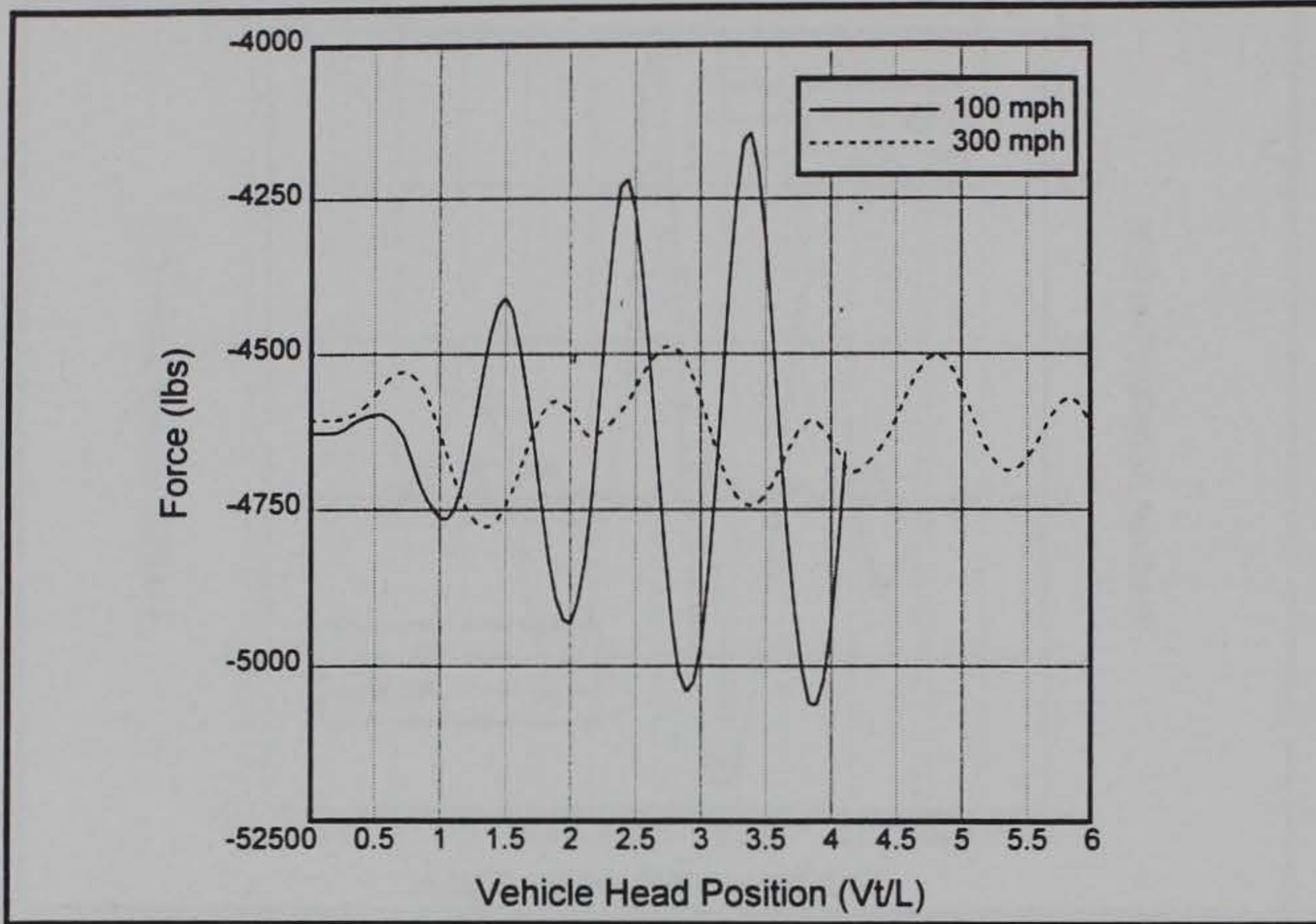


Figure 25. Spring force at vehicle's front (both springs)

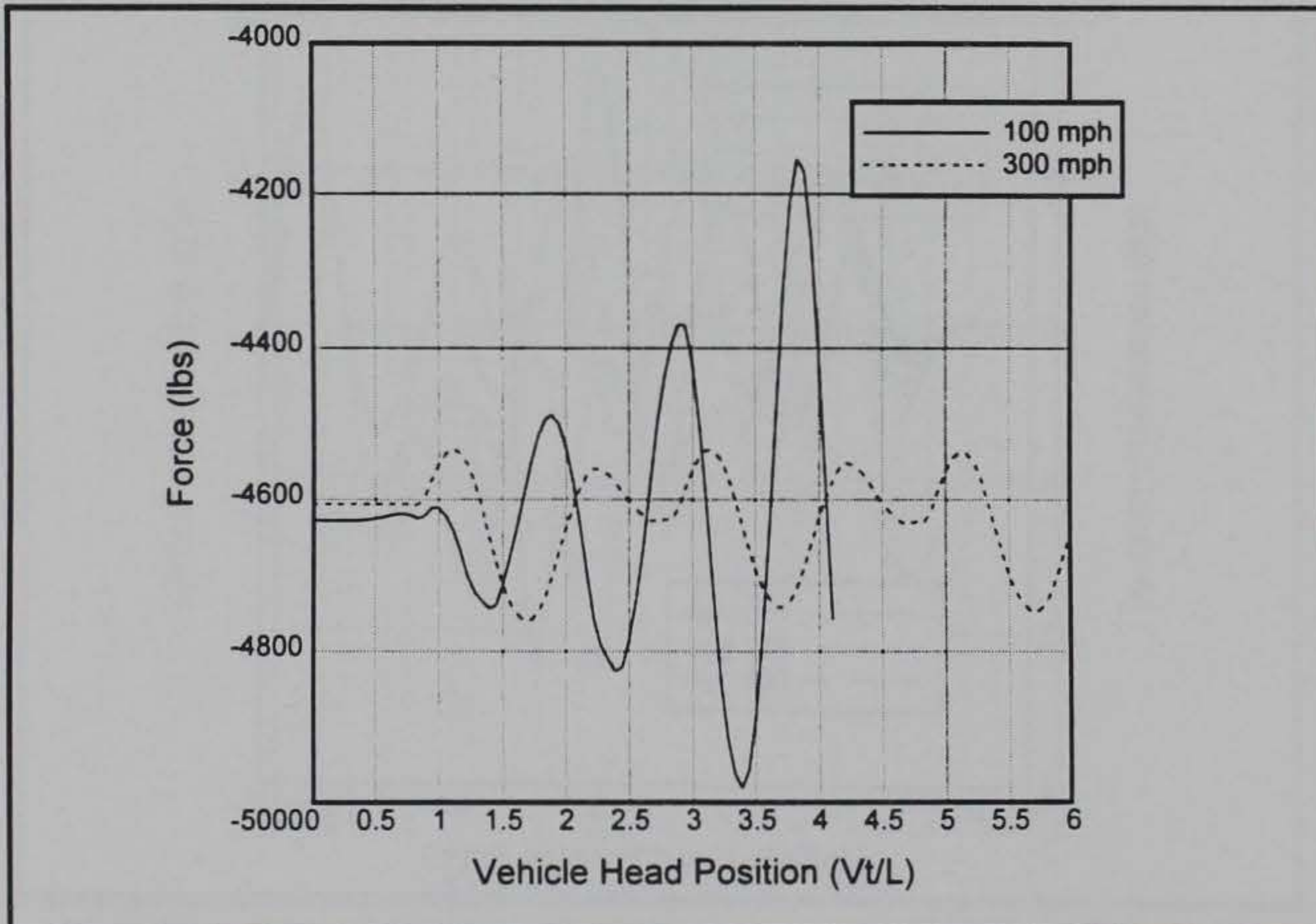


Figure 26. Spring force at vehicle's rear (both springs)

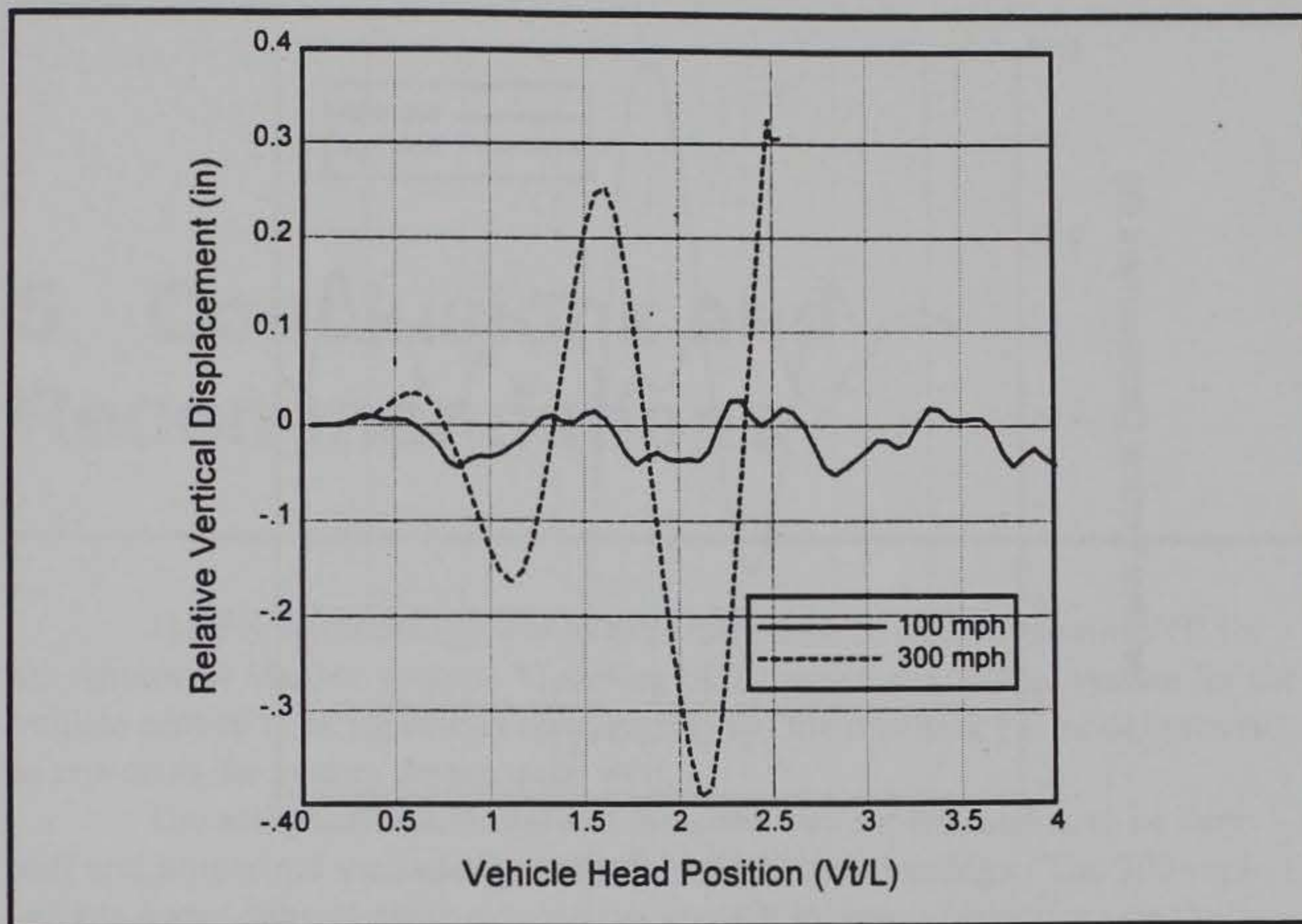


Figure 27. Magnetic gap variation at vehicle's front (linear spring only)

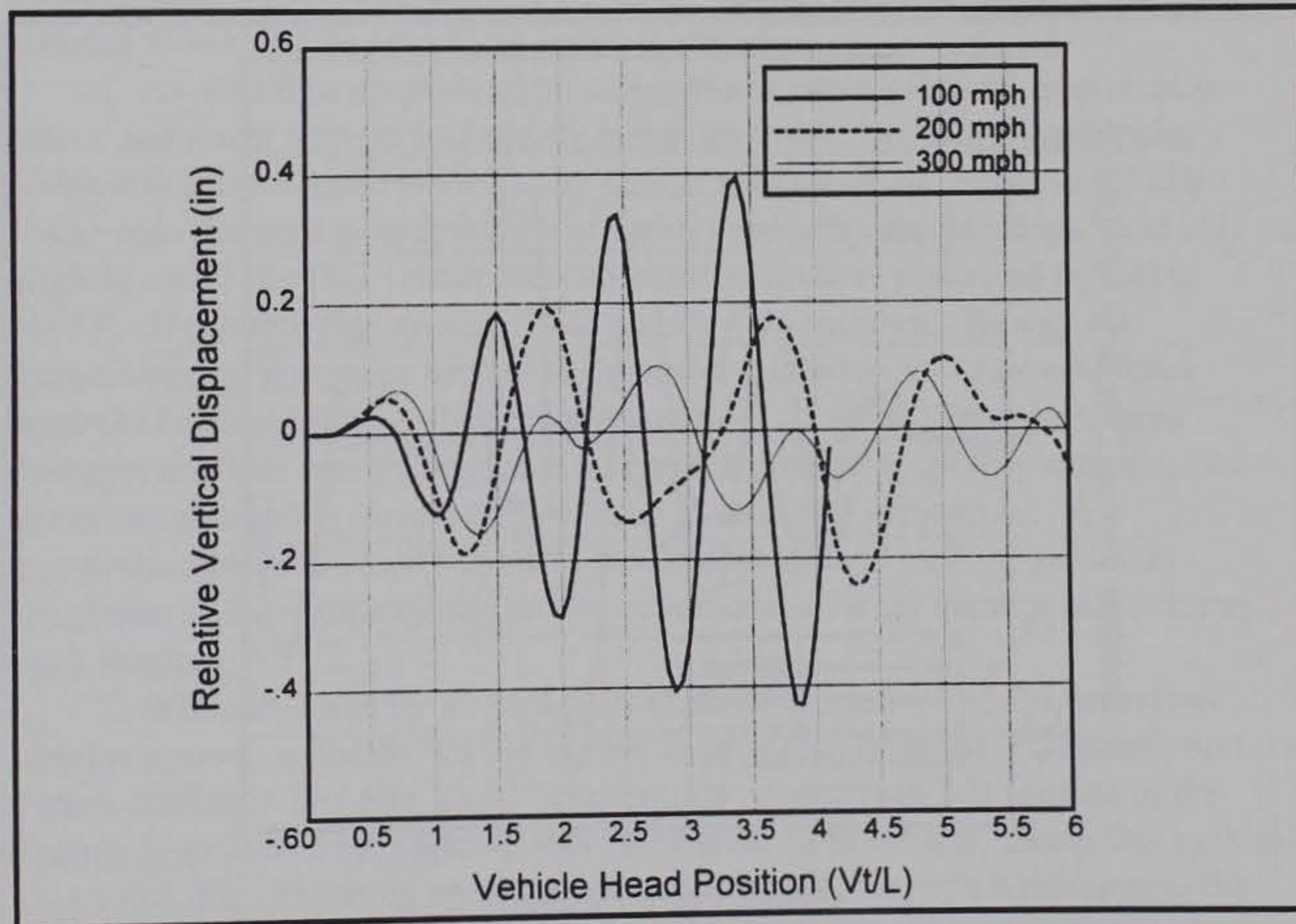


Figure 28. Magnetic gap variation at vehicle's front (both springs)

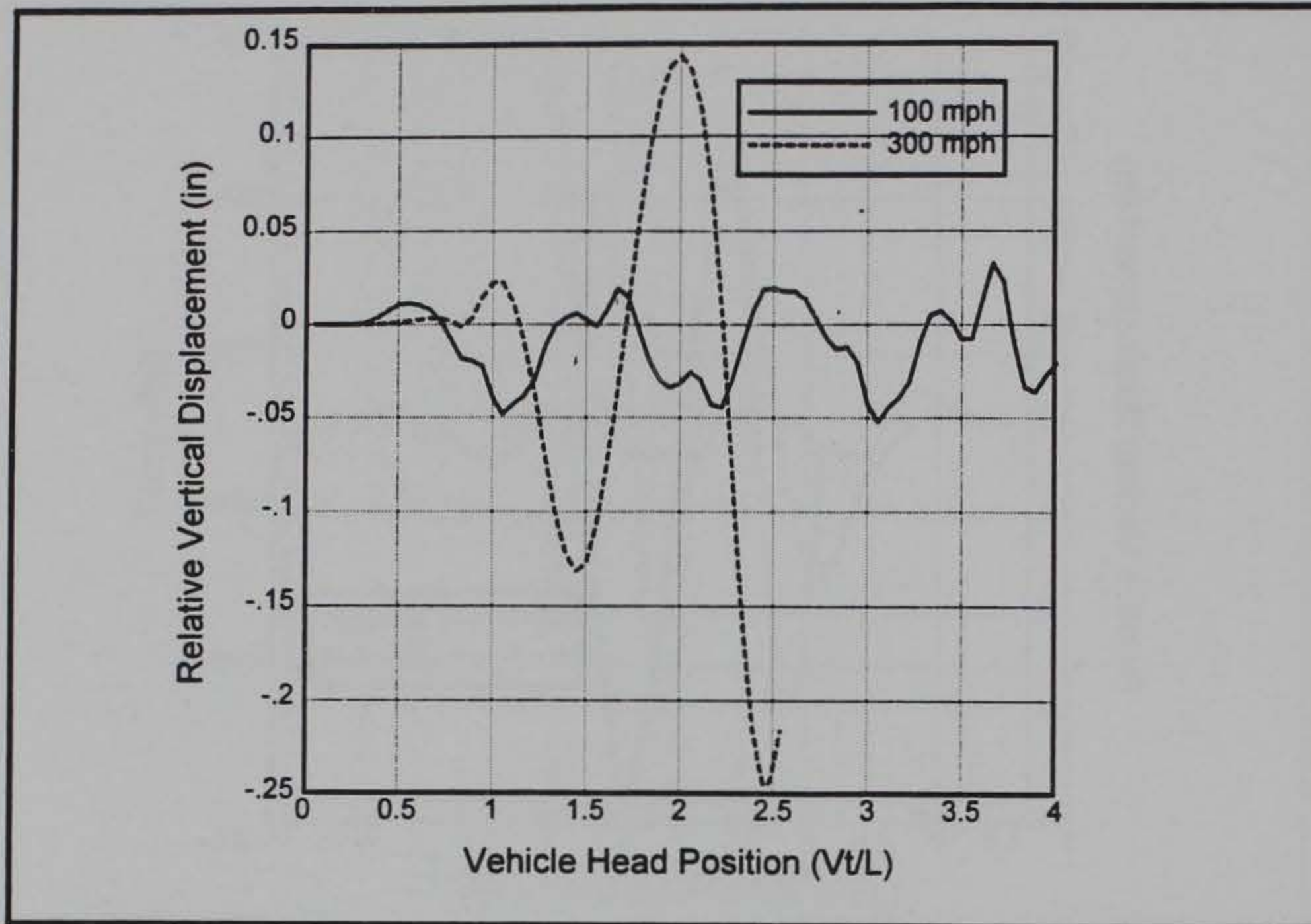


Figure 29. Magnetic gap variation at vehicle's rear (linear spring only)

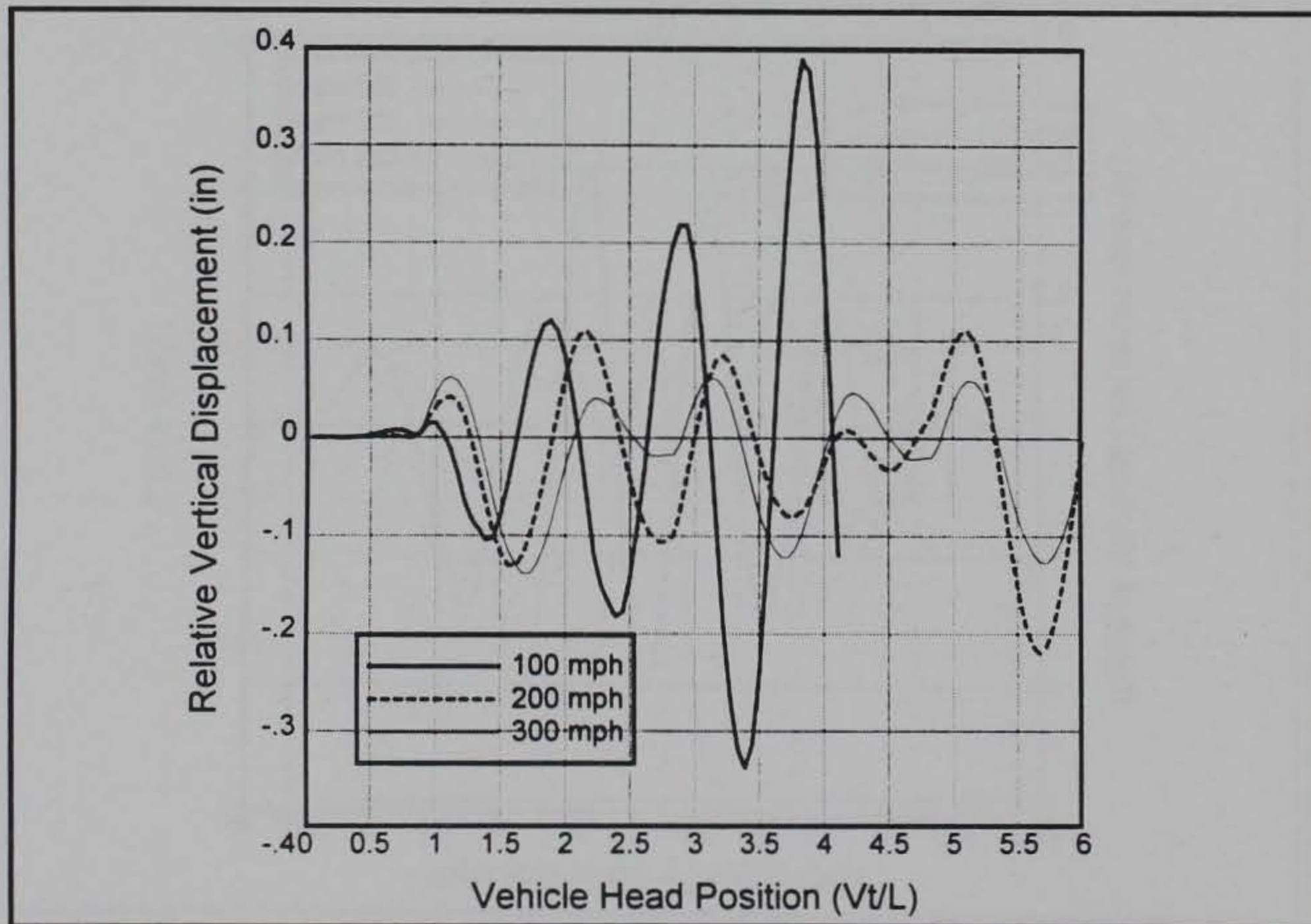


Figure 30. Magnetic gap variation at vehicle's rear (both springs)

5 Conclusions and Recommendations

The FE methodology was successfully used to study dynamic VGI for the American Maglev system. Modeling of the active suspension system for the vehicle proved to be especially challenging, but the resulting FE model proved to represent the system design quite well.

The analytical results showed the guideway superstructure to be very stiff and to respond well under the dynamic vehicular loadings. The 300-mph vehicle speed consistently produced the greatest midspan deflections on the guideway and indicated that a dynamic load factor of approximately 1.4 should be used for future guideway design applications with this system (assuming that both the active and linear suspensions are used on the vehicle). While no stress computations were made, the low guideway deflections indicate that high stresses should not be a problem in the guideway.

As would be suspected, the suspension system using the combination active and linear springs was clearly better from the ride quality standpoint. Vehicular accelerations were less by almost a factor of 10. However, while lower than the system with the linear springs only, the accelerations were still slightly above the ISO 1-hour reduced-comfort level as discussed by Lever (1993). If desired, ride quality could possibly be improved through the introduction of guideway precamber, a stiffer guideway, or improved force control characteristics for the active suspension. It should be remembered however that this was by no means a comprehensive ride quality analysis, and the comments above should only be used as an initial assessment. A comprehensive ride quality analysis would also include random guideway roughness and irregularity and would be run over a larger number of guideway span lengths.

While this was by no means an exhaustive analysis of the American Maglev system, it has shown the system to be viable from the VGI standpoint. Future studies in this area should concentrate on studying 3-D aspects of the dynamic response of the system, with emphasis on the vehicle. Since this system uses a null-flux levitation concept where the vehicle magnets wrap around the guideway coils, horizontal movements of the vehicle and horizontal magnetic gap variations will be very important. A 3-D analysis should consider wind, guidance, and centrifugal force effects on the vehicle and guideway. The effect

of these forces on the fiberglass railings (containing the guideway coils) should also be carefully studied.

References

Davey, K.R. (1994). Memorandum regarding specifications for vehicle spring constants, American Maglev Technology, Inc.

_____. (1995a). Memorandum regarding drawings of overall geometry of train, American Maglev Technology, Inc.

_____. (1995b). Memorandum regarding guideway details as related to the test sled, American Maglev Technology, Inc.

Grant, J.A. (1994). Memorandum regarding Maglev guideway structure, Grant/Holmberg Consultants, Inc.

Hibbitt, Karlsson and Sorensen, Inc. (1994). ABAQUS/Standard User's Manual, Release 5.4., Pawtucket, RI.

Lever, J. H. (1993). "Technical Assessment of Maglev System Concepts: Final Report by the Government Maglev System Assessment Team," U.S. Army Cold Regions Research and Engineering Laboratory, Hanover, NH.

Ray, J.C., Seda-Sanabria, Y., Chowdhury, M.R., and Woodson, S.C. (December 1995). "A Finite Element Model for Assessment of Maglev Vehicle/Guideway Interaction," Technical Report SL-95-23, U.S. Army Engineer Waterways Experiment Station, Vicksburg, MS.

335,	-194.,	48.
336,	-194.,	0.
337,	-214.,	0.
338,	-214.,	48.
339,	-402.,	48.
340,	-402.,	0.
341,	-422.,	48.
342,	-422.,	0.
343,	-442.,	48.
344,	-442.,	0.
345,	-462.,	0.
346,	-462.,	48.
347,	-618.,	48.
348,	-618.,	0.
349,	-638.,	48.
350,	-638.,	0.
351,	-658.,	48.
352,	-658.,	0.
353,	-678.,	0.
354,	-678.,	48.
355,	-866.,	48.
356,	-866.,	0.
357,	-886.,	48.
358,	-886.,	0.
359,	-906.,	48.
360,	-906.,	0.
361,	-926.,	0.
362,	-926.,	48.
363,	-1080.,	48.

**

**

**

Element Generation

**

=====

**

**

*ELEMENT, TYPE=B21

395,	329,	328
2,	328,	327
3,	327,	326
4,	326,	325
5,	325,	324
394,	324,	323
6,	323,	322

7,	322,	321
8,	321,	320
9,	320,	319
10,	319,	318
11,	318,	317
12,	317,	316
13,	316,	315
14,	315,	314
15,	314,	313
16,	313,	312
17,	312,	311
18,	311,	310
19,	310,	309
20,	309,	308
21,	308,	307
22,	307,	306
23,	306,	305
24,	305,	304
25,	304,	303
26,	303,	302
27,	302,	301
28,	301,	300
29,	300,	299
30,	299,	298
31,	298,	297
32,	297,	296
33,	296,	295
34,	295,	294
35,	294,	293
36,	293,	292
37,	292,	291
38,	291,	290
39,	290,	289
40,	289,	288
41,	288,	287
42,	287,	286
43,	286,	285
44,	285,	284
45,	284,	283
46,	283,	282
47,	282,	281
48,	281,	280
49,	280,	279
50,	279,	278
51,	278,	277

52,	277,	276
53,	276,	275
54,	275,	274
55,	274,	273
56,	273,	272
57,	272,	271
58,	271,	270
59,	270,	269
60,	269,	268
61,	268,	267
62,	267,	266
63,	266,	265
64,	265,	264
65,	264,	263
66,	263,	262
67,	262,	261
68,	261,	260
69,	260,	259
70,	259,	258
71,	258,	257
72,	257,	256
73,	256,	255
74,	255,	254
75,	254,	253
76,	253,	252
77,	252,	251
78,	251,	250
79,	250,	249
80,	249,	248
81,	248,	247
82,	247,	246
83,	246,	245
84,	245,	244
85,	244,	243
86,	243,	242
87,	242,	241
88,	241,	240
89,	240,	239
90,	239,	238
91,	238,	237
92,	237,	236
93,	236,	235
94,	235,	234
95,	234,	233
96,	233,	232

97,	232,	231
98,	231,	230
99,	230,	229
100,	229,	228
101,	228,	227
102,	227,	226
103,	226,	225
104,	225,	224
105,	224,	223
106,	223,	222
107,	222,	221
108,	221,	220
109,	219,	218
110,	218,	217
111,	217,	216
112,	216,	215
113,	215,	214
114,	214,	213
115,	213,	212
116,	212,	211
117,	211,	210
118,	210,	209
119,	209,	208
120,	208,	207
121,	207,	206
122,	206,	205
123,	205,	204
124,	204,	203
125,	203,	202
126,	202,	201
127,	201,	200
128,	200,	199
129,	199,	198
130,	198,	197
131,	197,	196
132,	196,	195
133,	195,	194
134,	194,	193
135,	193,	192
136,	192,	191
137,	191,	190
138,	190,	189
139,	189,	188
140,	188,	187
141,	187,	186

142,	186,	185
143,	185,	184
144,	184,	183
145,	183,	182
146,	182,	181
147,	181,	180
148,	180,	179
149,	179,	178
150,	178,	177
151,	177,	176
152,	176,	175
153,	175,	174
154,	174,	173
155,	173,	172
156,	172,	171
157,	171,	170
158,	170,	169
159,	169,	168
160,	168,	167
161,	167,	166
162,	166,	165
163,	165,	164
164,	164,	163
165,	163,	162
166,	162,	161
167,	161,	160
168,	160,	159
169,	159,	158
170,	158,	157
171,	157,	156
172,	156,	155
173,	155,	154
174,	154,	153
175,	153,	152
176,	152,	151
177,	151,	150
178,	150,	149
179,	149,	148
180,	148,	147
181,	147,	146
182,	146,	145
183,	145,	144
184,	144,	143
185,	143,	142
186,	142,	141

187,	141,	140
188,	140,	139
189,	139,	138
190,	138,	137
191,	137,	136
192,	136,	135
193,	135,	134
194,	134,	133
195,	133,	132
196,	132,	131
197,	131,	130
198,	130,	129
199,	129,	128
200,	128,	127
201,	127,	126
202,	126,	125
203,	125,	124
204,	124,	123
205,	123,	122
206,	122,	121
207,	121,	120
208,	120,	119
209,	119,	118
210,	118,	117
211,	117,	116
212,	116,	115
213,	115,	114
214,	114,	113
215,	113,	112
216,	112,	111
217,	110,	109
218,	109,	108
219,	108,	107
220,	107,	106
221,	106,	105
222,	105,	104
223,	104,	103
224,	103,	102
225,	102,	101
226,	101,	100
227,	100,	99
228,	99,	98
229,	98,	97
230,	97,	96
231,	96,	95

232,	95,	94
233,	94,	93
234,	93,	92
235,	92,	91
236,	91,	90
237,	90,	89
238,	89,	88
239,	88,	87
240,	87,	86
241,	86,	85
242,	85,	84
243,	84,	83
244,	83,	82
245,	82,	81
246,	81,	80
247,	80,	79
248,	79,	78
249,	78,	77
250,	77,	76
251,	76,	75
252,	75,	74
253,	74,	73
254,	73,	72
255,	72,	71
256,	71,	70
257,	70,	69
258,	69,	68
259,	68,	67
260,	67,	66
261,	66,	65
262,	65,	64
263,	64,	63
264,	63,	62
265,	62,	61
266,	61,	60
267,	60,	59
268,	59,	58
269,	58,	57
270,	57,	56
271,	56,	55
272,	55,	54
273,	54,	53
274,	53,	52
275,	52,	51
276,	51,	50

277,	50,	49
278,	49,	48
279,	48,	47
280,	47,	46
281,	46,	45
282,	45,	44
283,	44,	43
284,	43,	42
285,	42,	41
286,	41,	40
287,	40,	39
288,	39,	38
289,	38,	37
290,	37,	36
291,	36,	35
292,	35,	34
293,	34,	33
294,	33,	32
295,	32,	31
296,	31,	30
297,	30,	29
298,	29,	28
299,	28,	27
300,	27,	26
301,	26,	25
302,	25,	24
303,	24,	23
304,	23,	22
305,	22,	21
306,	21,	20
307,	20,	19
308,	19,	18
309,	18,	17
310,	17,	16
311,	16,	15
312,	15,	14
313,	14,	13
314,	13,	12
315,	12,	11
316,	11,	10
317,	10,	9
318,	9,	8
319,	8,	7
320,	7,	6
321,	6,	5

322,	5,	4
323,	4,	3
324,	3,	2
396,	2,	1
325,	331,	330
327,	333,	331
329,	335,	333
333,	338,	335
337,	339,	338
340,	341,	339
342,	343,	341
346,	346,	343
350,	347,	346
353,	349,	347
355,	351,	349
359,	354,	351
363,	355,	354
366,	357,	355
368,	359,	357
372,	362,	359
376,	363,	362

**

*ELEMENT, TYPE=SPRINGA

328,	331,	332
332,	333,	334
335,	335,	336
339,	337,	338
341,	339,	340
345,	341,	342
348,	343,	344
352,	345,	346
354,	347,	348
358,	349,	350
361,	351,	352
365,	353,	354
367,	355,	356
371,	357,	358
374,	359,	360
377,	361,	362

**

*ELEMENT, TYPE=SPRINGA

378,	331,	332
379,	333,	334
380,	335,	336
381,	337,	338


```

382,    339,    340
383,    341,    342
384,    343,    344
385,    345,    346
386,    347,    348
387,    349,    350
388,    351,    352
389,    353,    354
390,    355,    356
391,    357,    358
392,    359,    360
393,    361,    362

```

**

*ELEMENT, TYPE=ISL21

```

331,    334,    332
336,    337,    336
344,    342,    340
349,    345,    344
357,    350,    348
362,    353,    352
370,    358,    356
375,    361,    360

```

**

**

Grouping Nodes and Elements

**

=====

**

**

**

** Guideway

** -----

*NSET, NSET=GUIDEWAY

```

  2,    3,    4,    5,    6,    7,    8,    9,
10,   11,   12,   13,   14,   15,   16,   17,
18,   19,   20,   21,   22,   23,   24,   25,
26,   27,   28,   29,   30,   31,   32,   33,
34,   35,   36,   37,   38,   39,   40,   41,
42,   43,   44,   45,   46,   47,   48,   49,
50,   51,   52,   53,   54,   55,   56,   57,
58,   59,   60,   61,   62,   63,   64,   65,
66,   67,   68,   69,   70,   71,   72,   73,
74,   75,   76,   77,   78,   79,   80,   81,
82,   83,   84,   85,   86,   87,   88,   89,
90,   91,   92,   93,   94,   95,   96,   97,

```



```

98,    99,    100,   101,   102,   103,   104,   105,
106,   107,   108,   109,   110,   111,   112,   113,
114,   115,   116,   117,   118,   119,   120,   121,
122,   123,   124,   125,   126,   127,   128,   129,
130,   131,   132,   133,   134,   135,   136,   137,
138,   139,   140,   141,   142,   143,   144,   145,
146,   147,   148,   149,   150,   151,   152,   153,
154,   155,   156,   157,   158,   159,   160,   161,
162,   163,   164,   165,   166,   167,   168,   169,
170,   171,   172,   173,   174,   175,   176,   177,
178,   179,   180,   181,   182,   183,   184,   185,
186,   187,   188,   189,   190,   191,   192,   193,
194,   195,   196,   197,   198,   199,   200,   201,
202,   203,   204,   205,   206,   207,   208,   209,
210,   211,   212,   213,   214,   215,   216,   217,
218,   219,   220,   221,   222,   223,   224,   225,
226,   227,   228,   229,   230,   231,   232,   233,
234,   235,   236,   237,   238,   239,   240,   241,
242,   243,   244,   245,   246,   247,   248,   249,
250,   251,   252,   253,   254,   255,   256,   257,
258,   259,   260,   261,   262,   263,   264,   265,
266,   267,   268,   269,   270,   271,   272,   273,
274,   275,   276,   277,   278,   279,   280,   281,
282,   283,   284,   285,   286,   287,   288,   289,
290,   291,   292,   293,   294,   295,   296,   297,
298,   299,   300,   301,   302,   303,   304,   305,
306,   307,   308,   309,   310,   311,   312,   313,
314,   315,   316,   317,   318,   319,   320,   321,
322,   323,   324,   325,   326,   327,   328,   329,

```

**

*ELSET, ELSET=GUIDEWAY

```

2,    3,    4,    5,    6,    7,    8,    9,
10,   11,   12,   13,   14,   15,   16,   17,
18,   19,   20,   21,   22,   23,   24,   25,
26,   27,   28,   29,   30,   31,   32,   33,
34,   35,   36,   37,   38,   39,   40,   41,
42,   43,   44,   45,   46,   47,   48,   49,
50,   51,   52,   53,   54,   55,   56,   57,
58,   59,   60,   61,   62,   63,   64,   65,
66,   67,   68,   69,   70,   71,   72,   73,
74,   75,   76,   77,   78,   79,   80,   81,
82,   83,   84,   85,   86,   87,   88,   89,
90,   91,   92,   93,   94,   95,   96,   97,
98,   99,   100,  101,  102,  103,  104,  105,
106,  107,  108,  109,  110,  111,  112,  113,

```



```

114, 115, 116, 117, 118, 119, 120, 121,
122, 123, 124, 125, 126, 127, 128, 129,
130, 131, 132, 133, 134, 135, 136, 137,
138, 139, 140, 141, 142, 143, 144, 145,
146, 147, 148, 149, 150, 151, 152, 153,
154, 155, 156, 157, 158, 159, 160, 161,
162, 163, 164, 165, 166, 167, 168, 169,
170, 171, 172, 173, 174, 175, 176, 177,
178, 179, 180, 181, 182, 183, 184, 185,
186, 187, 188, 189, 190, 191, 192, 193,
194, 195, 196, 197, 198, 199, 200, 201,
202, 203, 204, 205, 206, 207, 208, 209,
210, 211, 212, 213, 214, 215, 216, 217,
218, 219, 220, 221, 222, 223, 224, 225,
226, 227, 228, 229, 230, 231, 232, 233,
234, 235, 236, 237, 238, 239, 240, 241,
242, 243, 244, 245, 246, 247, 248, 249,
250, 251, 252, 253, 254, 255, 256, 257,
258, 259, 260, 261, 262, 263, 264, 265,
266, 267, 268, 269, 270, 271, 272, 273,
274, 275, 276, 277, 278, 279, 280, 281,
282, 283, 284, 285, 286, 287, 288, 289,
290, 291, 292, 293, 294, 295, 296, 297,
298, 299, 300, 301, 302, 303, 304, 305,
306, 307, 308, 309, 310, 311, 312, 313,
314, 315, 316, 317, 318, 319, 320, 321,
322, 323, 324, 394,

```

**

** End of Guideway

** -----

*ELSET, ELSET=ENDTRACK

395, 396,

**

** Suspensions

** -----

*NSET, NSET=SPRINGS

```

331, 332, 333, 334, 335, 336, 337, 338,
339, 340, 341, 342, 343, 344, 345, 346,
347, 348, 349, 350, 351, 352, 353, 354,
355, 356, 357, 358, 359, 360, 361, 362,

```

**

*ELSET, ELSET=ACTSUSP

```

328, 332, 335, 339, 341, 345, 348, 352,
354, 358, 361, 365, 367, 371, 374, 377,

```

**


```

*ELSET, ELSET=PASSUSP
  378,  379,  380,  381,  382,  383,  384,  385,
  386,  387,  388,  389,  390,  391,  392,  393,
**
** Carbody
** -----
*NSET, NSET=CARBODY
  330,  331,  333,  335,  338,  339,  341,  343,
  346,  347,  349,  351,  354,  355,  357,  359,
  362,  363,
**
*ELSET, ELSET=CARBODY
  325,  327,  329,  333,  337,  340,  342,  346,
  350,  353,  355,  359,  363,  366,  368,  372,
  376,
**
** Set the EQUATION multi-point-constraints :
** -----
**
** *EQUATION
  2,
  331, 1, 1.0, 332, 1, -1.0
  2,
  333, 1, 1.0, 334, 1, -1.0
  2,
  335, 1, 1.0, 336, 1, -1.0
  2,
  338, 1, 1.0, 337, 1, -1.0
**
  2,
  339, 1, 1.0, 340, 1, -1.0
  2,
  341, 1, 1.0, 342, 1, -1.0
  2,
  343, 1, 1.0, 344, 1, -1.0
  2,
  346, 1, 1.0, 345, 1, -1.0
**
  2,
  347, 1, 1.0, 348, 1, -1.0
  2,
  349, 1, 1.0, 350, 1, -1.0
  2,
  351, 1, 1.0, 352, 1, -1.0
  2,

```



```

354, 1, 1.0, 353, 1, -1.0
**
2,
355, 1, 1.0, 356, 1, -1.0
2,
357, 1, 1.0, 358, 1, -1.0
2,
359, 1, 1.0, 360, 1, -1.0
2,
362, 1, 1.0, 361, 1, -1.0
**
** Slide Line Magnets
** -----
*NSET, NSET=MAGNETS
332, 334, 336, 337, 340, 342, 344, 345,
348, 350, 352, 353, 356, 358, 360, 361
**
*ELSET, ELSET=MAGNETS
331, 336, 344, 349, 357, 362, 370, 375
**
** Slide Lines
** -----
*SLIDE LINE, ELSET=MAGNETS, TYPE=LINEAR, GENERATE,
SMOOTH=0.2
329, 329, 0
328, 274, -1
273, 220, -1
219, 165, -1
164, 111, -1
110, 56, -1
55, 2, -1
1, 1, 0
**
*****
**
** Element Properties
** =====
**
*****
**
** Guideway
** -----
*BEAM SECTION, SECT=RECT, MATERIAL=GUIDEMAT, ELSET=GUIDEWAY
96., 63.
0., 0., -1.

```



```

**
** End of Guideway
** -----
** BEAM SECTION, SECT=RECT, MATERIAL=ENDMAT, ELSET=ENDTRACK
24.,8.
0., 0., -1.
** Suspensions
** -----
** (ACTIVE LIFT COILS) --> All Stiff. K = Ko * 2
** =====
** SPRING, ELSET=ACTSUSP, NONLINEAR
,,
-5599.2,      -1.8
-5586.5936,   -1.7
-5565.3408,   -1.6
-5535.6912,   -1.5
-5497.8944,   -1.4
-5452.2,      -1.3
-5398.8576,   -1.2
-5338.1168,   -1.1
-5270.2272,   -1.0
-5195.4384,   -0.9
-5114.0,      -0.8
-5026.1616,   -0.7
-4932.1728,   -0.6
-4832.2832,   -0.5
-4726.7424,   -0.4
-4615.8,      -0.3
-4499.7056,   -0.2
-4378.7088,   -0.1
-4253.0592,    0.0
-4123.0064,    0.1
-3988.8,       0.2
-3850.6896,    0.3
-3708.9248,    0.4
-3563.7552,    0.5
-3415.4304,    0.6
-3264.2,       0.7
-3110.3136,    0.8
-2954.0208,    0.9
-2795.5712,    1.0
-2635.2144,    1.1
-2473.2,       1.2
-2309.7776,    1.3
-2145.1968,    1.4

```



```

-1979.7072, 1.5
-1813.5584, 1.6
-1647.0, 1.7
-1480.2816, 1.8
-1313.6528, 1.9
-1147.3632, 2.0
-981.6624, 2.1
-816.8, 2.2
-653.0256, 2.3
-490.5888, 2.4
-329.7392, 2.5
-170.7264, 2.6
-13.8, 2.7
140.7904, 2.8
292.7952, 2.9
441.9648, 3.0
588.0496, 3.1
730.8, 3.2
869.9664, 3.3
1005.2992, 3.4
1136.5488, 3.5
1263.4656, 3.6
1385.8, 3.7
1503.3024, 3.8
1615.7232, 3.9
1722.8128, 4.0
1824.3216, 4.1
1920.0, 4.2
2302.2, 4.3
2501.2, 4.4

```

```

**
** (COMPOSITE COILS) --> Stiff Ko=664.55 lb/in * 2 sides
** ======> 1329.1 lb/in
**
*SPRING, ELSET=PASSUSP

```

```
1329.1,
```

```
**
```

```
** Carbody
```

```
** -----
```

```
*BEAM SECTION, SECT=RECT, MATERIAL=VEHICMAT, ELSET=CARBODY
```

```
96.,96.
```

```
0., 0., -1.
```

```
**
```

```
** Slide Line Magnets
```

```
** -----
```



```

*INTERFACE, ELSET=MAGNETS
1., 0.,0.,1.
*FRICTION
0.3
**
*****
**
**                               Material Properties
**                               =====
**
*****
**
** Guideway Material
** -----
**
** *MATERIAL, NAME=GUIDEMAT
** *DENSITY
** 0.0000992063,
** *ELASTIC, TYPE=ISO
** 4888.E+03, 0.15
** *TRANSVERSE SHEAR STIFFNESS
** 2.17E+06
**
** End Track Material
** -----
**
** *MATERIAL, NAME=ENDMAT
** *DENSITY
** 1E-6,
** *ELASTIC, TYPE=ISO
** 30.E6, 0.3
**
** Carbody
** -----
**
** *MATERIAL, NAME=VEHICMAT
** *DENSITY
** 0.000020797
** *ELASTIC, TYPE=ISO
** 30.E+10
**
*****
**
**                               Boundary Conditions
**                               =====
**
*****
**

```



```

** Hinges
** -----
*BOUNDARY
    56, 1,2
    165, 1,2
    274, 1,2
**
** Rollers
** -----
*BOUNDARY
    2, 2,2
**
    110, 2,2
    111, 2,2
**
    219, 2,2
    220, 2,2
**
    328, 2,2
**
** Fixed-Ends
** -----
*BOUNDARY
    1, 1,2
    329, 1,2
**
    330, 1,1
    332, 1,1
**
SPRINGS, 3, 3
**
**
**
**
**
**
*****
**
**                               Output Request
**                               =====
**
*****
**
** Applying Initial Displacement on Springs
** -----

```



```

*STEP, AMPLITUDE=STEP
*STATIC
0.05,1.0,0.05
*BOUNDARY
CARBODY,2,2,-0.289
**
** Self Weight of the Vehicle and Guideway
** -----
*DLOAD
CARBODY, GRAV, 386.21, 0.,-1.,0.
GUIDEWAY, GRAV, 386.21, 0.,-1.,0.
**
** Distributed Load Along Guideway (to consider pre-
    stressing effect)
** -----
*DLOAD
GUIDEWAY,PY,231.67
**
*NODE FILE
U
RF
*EL FILE, ELSET=PASSUSP
S
*EL FILE, ELSET=ACTSUSP
S
*NODE PRINT, F=0
*EL PRINT, F=0
*END STEP
**
** Equilibrating the system
** -----
*STEP, AMPLITUDE=STEP
*STATIC
*BOUNDARY, OP=NEW
    56, 1,2
    165, 1,2
    274, 1,2
    2, 2,2
    110, 2,2
    111, 2,2
    219, 2,2
    220, 2,2
    328, 2,2
    1, 1,2
    329, 1,2

```



```

        330, 1,1
        332, 1,1
SPRINGS, 3,3
*NODE FILE
U
RF
*EL FILE, ELSET=PASSUSP
S
*EL FILE, ELSET=ACTSUSP
S
*NODE PRINT, F=0
*EL PRINT, F=0
*END STEP
**
** Dynamic Analysis of the System (Velocity = 300 mph
   [5275.58 in/sec])
** -----
*STEP, INC=500
*DYNAMIC, DIRECT, NOHAF
0.003791, 1.4330
*RESTART, WRITE, FREQ=3
*PRINT, CONTACT=YES
*NSET, NSET=MAGLEV
MAGNETS, 330, 363
*BOUNDARY, OP=NEW
    56, 1,2
    165, 1,2
    274, 1,2
    2, 2,2
    110, 2,2
    111, 2,2
    219, 2,2
    220, 2,2
    328, 2,2
    1, 1,2
    329, 1,2
SPRINGS, 3,3
*BOUNDARY, TYPE=VELOCITY, OP=NEW
MAGLEV, 1, 1, 5275.58
*NODE FILE, FREQ=3
U
V
A
RF
*EL FILE, FREQ=3, ELSET=PASSUSP

```



```
S
*EL FILE, FREQ=3, ELSET=ACTSUSP
S
*FILE FORMAT, ASCII
*NODE PRINT, F=0
*EL PRINT, F=0
*END STEP
```


REPORT DOCUMENTATION PAGE

Form Approved
OMB No. 0704-0188

Public reporting burden for this collection of information is estimated to average 1 hour per response, including the time for reviewing instructions, searching existing data sources, gathering and maintaining the data needed, and completing and reviewing the collection of information. Send comments regarding this burden estimate or any other aspect of this collection of information, including suggestions for reducing this burden, to Washington Headquarters Services, Directorate for Information Operations and Reports, 1215 Jefferson Davis Highway, Suite 1204, Arlington, VA 22202-4302, and to the Office of Management and Budget, Paperwork Reduction Project (0704-0188), Washington, DC 20503.

1. AGENCY USE ONLY (Leave blank)		2. REPORT DATE June 1996	3. REPORT TYPE AND DATES COVERED Final report	
4. TITLE AND SUBTITLE Dynamic Analysis of the American Maglev System			5. FUNDING NUMBERS	
6. AUTHOR(S) Yazmin Seda-Sanabria, James C. Ray				
7. PERFORMING ORGANIZATION NAME(S) AND ADDRESS(ES) U.S. Army Engineer Waterways Experiment Station 3909 Halls Ferry Road, Vicksburg, MS 39180-6199			8. PERFORMING ORGANIZATION REPORT NUMBER Technical Report SL-96-10	
9. SPONSORING/MONITORING AGENCY NAME(S) AND ADDRESS(ES) U.S. Army Engineer Division, Huntsville P.O. Box 1600, Huntsville, AL 35807-4301			10. SPONSORING/MONITORING AGENCY REPORT NUMBER	
11. SUPPLEMENTARY NOTES Available from National Technical Information Service, 5285 Port Royal Road, Springfield, VA 22161.				
12a. DISTRIBUTION/AVAILABILITY STATEMENT Approved for public release; distribution is unlimited.			12b. DISTRIBUTION CODE	
13. ABSTRACT (Maximum 200 words) Understanding the dynamic interaction between a magnetic levitated (Maglev) vehicle and its supporting guideway is essential in the evaluation of the performance of such a system. This interacting coupling, known as vehicle/guideway interaction (VGI), has a significant effect on system parameters such as the required magnetic suspension forces and gaps, vehicular ride quality, and guideway deflections and stresses. This report presents the VGI analyses conducted on an actual Maglev system concept definition (SCD), the American Maglev SCD, using a linear-elastic finite-element (FE) model. Particular interest was focused on the comparison of the ride quality of the vehicle, using two different suspension systems, and their effect on the guideway structure. The procedure and necessary assumptions in the modeling are discussed.				
14. SUBJECT TERMS High-speed ground transportation Maglev Magnetic levitation Vehicle/guideway interaction			15. NUMBER OF PAGES 61	
			16. PRICE CODE	
17. SECURITY CLASSIFICATION OF REPORT UNCLASSIFIED	18. SECURITY CLASSIFICATION OF THIS PAGE UNCLASSIFIED	19. SECURITY CLASSIFICATION OF ABSTRACT	20. LIMITATION OF ABSTRACT	